



PERFORMANCE STUDY OF STAGING VARIABLES ON TWO-STAGE-TO-ORBIT REUSABLE LAUNCH VEHICLES

THESIS

James K. Nilsen, 1st Lieutenant, USAF
AFIT/GA/ENY/05-M08

**DEPARTMENT OF THE AIR FORCE
AIR UNIVERSITY
*AIR FORCE INSTITUTE OF TECHNOLOGY***

Wright-Patterson Air Force Base, Ohio

APPROVED FOR PUBLIC RELEASE; DISTRIBUTION UNLIMITED

The views expressed in this thesis are those of the author and do not reflect the official policy or position of the United States Air Force, Department of Defense, or the United States Government.

AFIT/GA/ENY/05-M08

PERFORMANCE STUDY OF STAGING VARIABLES ON TWO-STAGE-TO-ORBIT
REUSABLE LAUNCH VEHICLES

THESIS

Presented to the Faculty

Department of Aeronautics and Astronautics

Graduate School of Engineering and Management

Air Force Institute of Technology

Air University

Air Education and Training Command

In Partial Fulfillment of the Requirements for the
Degree of Master of Science in Astronautical Engineering

James K. Nilsen, BS

1st Lieutenant, USAF

March 2005

APPROVED FOR PUBLIC RELEASE; DISTRIBUTION UNLIMITED.

AFIT/GA/ENY/05-M08

PERFORMANCE STUDY OF STAGING VARIABLES ON TWO-STAGE-TO-ORBIT
REUSABLE LAUNCH VEHICLES

James K. Nilsen, BS
1st Lieutenant, USAF

Approved:

Milton E. Franke (Chairman)

date

Ralph A. Anthenien (Member)

date

Paul L. King (Member)

date

Abstract

The purpose of this research is to investigate the effects of staging variables on Two-Stage-To-Orbit reusable launch vehicles, specifically, the question of what measurable factors play important roles in staging performance. Three different configurations (Rocket-Rocket, Turbojet-Rocket and Turbine Based Combined Cycle-Rocket) were considered. The software, Program to Optimize Simulated Trajectories (POST), was used to analyze these configurations. Vehicle coasting time, staging dynamic pressure and staging Mach number were all varied to determine their influence on the final payload.

The results of the computational code runs provide data that support the need to develop tools and procedures to better understand high dynamic pressure staging. This could result in an increased payload weight for air-breathing launch vehicles. As staging dynamic pressures for the air-breathing vehicles were increased, so did the final payload weight. In traditional rocket configurations, the final payload weight increased as the dynamic pressure at staging decreased.

Acknowledgments

I would like to express my sincere appreciation to my faculty advisor, Dr. Milton Franke, for his guidance and support throughout the course of this thesis effort. The insight and experience was certainly appreciated. I would, also, like to thank my sponsor, Lt. Jack Barnett, from the Air Force Research Laboratory for both the support and latitude provided to me in this endeavor.

I am also indebted to Mr. Chan Cho, from the Air Force Research Laboratory, whose knowledge of POST was invaluable. I am also indebted to my fellow Astronautical Engineering students who helped me to not only endure AFIT, but to enjoy the experience, as a whole.

Finally, I must thank my wife and children for supporting me the past 18 months. My family constantly reminded me to keep things in perspective, gave me support and offered me time to relax. Thank you.

James K. Nilsen

Table of Contents

| | Page |
|--|------|
| Abstract | iv |
| Acknowledgements | v |
| Table of Contents | vi |
| List of Figures | viii |
| List of Tables | ix |
| List of Symbols | x |
| I. Introduction | 1 |
| Background..... | 1 |
| Research Objective | 3 |
| Thesis Overview | 3 |
| II. Literature Review | 5 |
| Prior Thesis Work..... | 5 |
| NASA Scramjet Project | 5 |
| NASA Staging Research..... | 6 |
| Proposed RLV Designs..... | 7 |
| III. Methodology | 11 |
| Program to Optimize Simulated Trajectories | 11 |
| Input Files | 13 |
| Parameters..... | 14 |
| Pitch Control | 22 |
| Payload..... | 22 |
| Accuracy Assessment | 23 |
| IV. Results and Analysis..... | 25 |
| Configurations..... | 25 |
| Coasting Time | 30 |
| Dynamic Pressure | 36 |
| Mach Number | 41 |

| | Page |
|--|------|
| V. Conclusions and Recommendations | 46 |
| Coasting Conclusions..... | 46 |
| Dynamic Pressure Conclusions..... | 46 |
| Mach number Conclusions | 46 |
| Final Recommendations..... | 47 |
| Appendix A: X-43 Aerodynamic Properties..... | 48 |
| Bibliography | 51 |
| Vita..... | 53 |

List of Figures

| | Page |
|---|------|
| Figure 1. Quicksat weight as a function of maximum scramjet Mach number and staging velocity..... | 10 |
| Figure 2. Altitude profile for the RKT configuration as generated by POST..... | 25 |
| Figure 3. Altitude profile for the TJ configuration as generated by POST..... | 27 |
| Figure 4. Thrust minus drag vs. weight for baseline TBCC (lbf)..... | 28 |
| Figure 5. Altitude profile for the TBCC configuration as generated by POST..... | 29 |
| Figure 6. Altitude profile as coasting time increases (TJ configuration)..... | 33 |
| Figure 7. Comparison of altitude profiles for baseline configurations as generated by POST..... | 35 |
| Figure 8. Altitude profile for the TJ configuration as staging dynamic pressure varies.. | 37 |
| Figure 9. Altitude profile for the TBCC configuration as staging dynamic pressure varies..... | 38 |
| Figure 10. Final payload (stage 3) weight as a function of staging dynamic pressure | 39 |
| Figure 11. Percent Change in total stage weight from baseline TBCC configuration as staging dynamic pressure varies | 40 |
| Figure 12. Change in total stage weight from baseline TJ configuration as staging dynamic pressure varies..... | 40 |
| Figure 13. Payload weight for RKT configurations including Brock data (1:55)..... | 42 |
| Figure 14. Altitude profile as staging Mach number varies for RKT configurations..... | 43 |
| Figure 15. Comparison of staging dynamic pressures vs. staging Mach number..... | 45 |

List of Tables

| | Page |
|---|------|
| Table 1. Spaceworks Study of Maximum Scramjet Mach Number | 10 |
| Table 2. Summary of Varied Parameters..... | 15 |
| Table 3. AFRL Mach 4.4 Turbojet Thrust (lbf)..... | 18 |
| Table 4. AFRL Mach 4.4 Turbojet Isp (sec)..... | 18 |
| Table 5. Hypersonic Research Engine-Scramjet Data..... | 20 |
| Table 6. Results of Baseline Configurations..... | 30 |
| Table 7. Coasting Time Effect on Payload (without fixed altitudes) | 31 |
| Table 8. Variation in Staging Conditions as Coasting Time Increased | 32 |
| Table 9. Coasting Time Effects on Payload (with fixed altitudes)..... | 34 |

List of Symbols

| | |
|-------|---|
| AFRL | Air Force Research Laboratory |
| Alt | Altitude |
| DYNP | Dynamic pressure $\frac{1}{2}\rho v^2$ (psf) |
| F | Inert mass fraction |
| HTHL | Horizontal takeoff horizontal landing |
| Isp | Specific impulse (sec) |
| Mach | Mach number |
| Mi | Inert weight (lbm) |
| Mpay | Payload weight (lbm) |
| Mprop | Stage propellant weight (lbm) |
| NASA | National Air and Space Agency |
| psf | Pounds force per square foot (lbf/ft ²) |
| RKT | Rocket-rocket |
| RLV | Reusable launch vehicle |
| TBCC | Turbine based combined cycle-rocket |
| TJ | Turbojet-rocket |
| TSTO | Two-Stage-To-Orbit |
| T/W | Thrust to weight |
| USAF | United States Air Force |
| VTHL | Vertical takeoff horizontal landing |
| VTVL | Vertical takeoff vertical landing |

PERFORMANCE STUDY OF STAGING VARIABLES ON TWO-STAGE- TO-ORBIT REUSABLE LAUNCH VEHICLES

I. Introduction

Background

The United States Air Force (USAF) and the National Air and Space Agency (NASA) are both seeking designs that lead to inexpensive access to space. As NASA prepares for the retirement of the Space Shuttle in 2010, the USAF is investigating new, on-demand reusable launch vehicles (RLV). With the successful completion of the Ansari X prize competition by Burt Rutan and his "Spaceship One," and the commencement of the "America's Space Prize" (8:87) competition, it is apparent that private industry is also seeking an inexpensive RLV.

New designs promise everything from long range missiles to air-breathing RLV. One design commonality is the scramjet engine. Scramjets, and other air-breathing engines, extract the oxidizer needed for combustion from the ambient air flow around the vehicle. This provides an increase in engine efficiency, characterized by specific impulse (Isp), and the overall vehicle weight savings. The drawback to using scramjets and other air-breathing engines have a limited range of operability. Turbojets, for example, have an operational range of Mach 0 to about Mach 4.4. This turbojet Mach number comes from data provided by AFRL from the conceptual Mach 4.4 turbine accelerator design (1:42). Another example is that ramjets operate from about Mach 1 to about Mach 7, with a

specific thrust maximum at about Mach 3 (10:163). Scramjets, on the other hand, operate from about Mach 4 to about Mach 8. These scramjet operational limits are based on the Hypersonic Research Engine (HRE) data provided by AFRL (1).

The main difference between ramjet and scramjet engines is that in a scramjet engine the supersonic air flow is sustained throughout the engine. A limitation to air-breathing ram compression propulsion is the need for high dynamic pressure (greater than 1000 psf) in the external free stream. This high dynamic pressure is needed to compress the working fluid (air).

Lift, drag and externally applied moments are all dependant on dynamic pressure. Lift and drag are calculated based on the dynamic pressure, the surface area, and the effective lift and drag coefficients. The drag applied to a vehicle is higher in a high dynamic pressure environment than a low dynamic pressure environment. The dynamic pressure encountered during vehicle separation provides an estimate on the forces encountered during separation. For example, the external moments due to changes in the air flow generated by separation are higher in a high dynamic pressure environment than in a low dynamic pressure environment.

When a Pegasus booster rocket separates from a B-52 wing; this process would be considered staging. In addition, the transition from turbine engine only to rocket booster assist is not considered staging since no physical separation occurs. Another example is in a Two-Stage-To-Orbit (TSTO) launch vehicle concept, the separation of the two stage configuration to upper stage configuration is considered staging. For the purpose of this study, staging is defined as the physical separation of two parts of a launch vehicle from one another.

The Space Shuttle and other rocket configurations stage at medium (less than 1000 psf) to low (less than 100 psf) dynamic pressures, due to the direct ascent trajectory taken by these vehicles. In the direct ascent trajectory, the air density decreases too rapidly to achieve high dynamic pressure conditions. Final payload insertion occurs at a very low dynamic pressure (less than 1 psf). This is due to the low air density at the altitude where final payload insertion occurs. Traditional rockets minimize aerodynamic effects applied to the upper stage by stacking one stage on top of the next.

Some RLV concepts being developed use neither a stacking method, nor a direct ascent trajectory to minimize aerodynamic effects on the upper stage. To minimize the aerodynamic effects during separation, designers and engineers of these new RLV concepts force their designs to separate at low dynamic pressures.

Research Objective

By studying air-breathing vehicles and their interaction with various dynamic pressures, this research will specify the effect on payload weight of stage separation in at various dynamic pressure environments. Some studies neglect to include coasting time in the stage separation process. This research will examine the effect of coasting time on the final payload weight. Furthermore, traditional rocket vehicles use Mach number as a staging parameter. Dynamic pressure data has been extracted from Mach number studies as a way of comparing traditional rocket configurations to air-breathing configurations.

Thesis Overview

This work is organized into five chapters and one appendix. Chapter II contains a literature review on the background of physical staging in high dynamic pressure environments. Chapter III provides the methodology and a description of the computer

program used throughout the research process. Chapter IV presents the results of the research. Chapter V provides conclusions for these results and recommends future analysis. Appendix A presents the aerodynamic properties of the X-43, Hyper-X.

II. Literature Review

Prior Work

The groundwork for this research is a study conducted by Marc A. Brock in 2004 titled *Performance Study of Two-Stage-Two Orbit Reusable Launch Vehicle Propulsion Alternatives* (1). The work studied five Two-Stage-To-Orbit (TSTO) reusable launch vehicles (RLV) using different configurations of rocket, turbojet and scramjet engines along with different ascent trajectories and inert mass fractions. Brock used a computer program developed by NASA to analyze and compare different configurations, called Program to Optimize Simulated Trajectories (POST).

Brock found that the turbojet-rocket (TJ) configuration was “insensitive to 1st stage weight fractions” (1). Meaning that given a fixed takeoff weight the final payload increased as first stage inert mass fraction increased as much as 15% above the lowest inert mass fraction calculated for the TJ configuration (1:68). Secondly, the payload capacities for air-breathing turbojet rocket configurations with horizontal takeoffs were three times as great compared to vertical takeoffs. Brock recommended that further study of the turbojet and turbine-based combined cycle engines in lifting trajectories be conducted (1).

NASA Scramjet Project

The X-43 (Hyper-X) hypersonic demonstrator developed by NASA is an exceptional platform for information, specifically regarding staging (3). Since the Hyper-X was to test a scramjet engine in a hypersonic live-fire test, the test vehicle was accelerated up to a high dynamic pressure environment before separation from its

Pegasus booster rocket. Even though the Hyper-X was mounted in a stacked configuration with the Pegasus booster, the mating adaptor that attached the Hyper-X to the Pegasus booster created an overlap that generated two unsteady aerodynamic effects. The first was during initial separation where the “establishment of quasi-steady flow in the gap that opens up between the research vehicle and the adapter” (4:2). The second came from the hypersonic fluid flow around the vehicles as separation continued (4:2).

Another issue for NASA was that “there has never been a successful separation of two vehicles (let alone a separation of two non-axisymmetric vehicles)” (3:1) at the stage separation conditions planned for the Hyper-X. The Hyper-X stages at Mach 7, at an altitude of about 95,000 ft, with a staging dynamic pressure of approximately 1000 psf (4:1). Most of the work done on the Hyper-X, prior to the first flight in 2000, was centered on predicting and controlling the aerodynamic effects created during staging. Wind tunnel tests were conducted and computational fluid dynamic (CFD) models were generated to try to predict the flow around the test vehicle and booster rocket during staging. Several concepts have been tested and reviewed to minimize the interference generated by the fluid flow around each vehicle while in the process of separating (5).

The Hyper-X succeeded in its first successful powered flight in March 2004, where it broke the speed record for air-breathing vehicles. It broke the same record months later in November 2004 when it flew at Mach 9.8.

NASA Staging Research

NASA is continuing the research in the field of high dynamic pressure separation. NASA Langley Research Center in Hampton, VA where studies are underway to help understand aerodynamic issues involved with stage separation (2). By developing a

framework for building CFD and wind tunnel test models, the studies will establish a database for staging at high dynamic pressures. To date, only one configuration has been studied by NASA Langley. The architecture used does allow for adaptation to new configurations. A promising item regarding the research is the ability to generate data for the given configuration at different positions and orientations.

Proposed RLV Designs

SpaceWorks Engineering, Inc. (Spaceworks), a private firm, based in Atlanta, GA is conducting a study for the Propulsion Directorate, Air Force Research Laboratory (AFRL), Wright-Patterson Air Force Base, OH. The study is investigating a responsive and a multi-mission capable TSTO RLV, called Quicksat (6). With the intention of validating their configurations for Quicksat, Spaceworks uses POST to develop an optimized trajectory.

The first stage of Quicksat is a reusable horizontal takeoff horizontal landing (HTHL) booster powered by six turbine engines, four tail rockets and a scramjet engine. The proposed trajectory for Quicksat follows a 2000 psf dynamic pressure profile, as it operates in scramjet mode, to approximately 100,000 ft traveling at Mach 8. Quicksat then performs a pull-up maneuver followed by the dynamic pressure dropping to about 500 psf (6:9). Instead of staging, the four tail rockets are fired to propel the vehicle from approximately 100,000 ft to about 250,000 ft thereby lowering the dynamic pressure to about 25 psf. The second stage rocket and payload separate from the first stage booster and the first stage booster returns to the originating airfield using its turbine engines.

Quicksat takes advantage of several new technologies, including scramjet engines, carbon composite lifting body structures, and horizontal takeoffs and landings.

A drawback to Quicksat is the complex engine configuration (with six turbojet engines, a scramjet engine and four tail rockets on the first stage booster) is the amount of engine maintenance needed to certify the vehicle for flight after each mission. Provided that the maintenance needs are addressed and the technologies needed are developed, the Quicksat concept could provide the USAF with a capable, on-demand, multi-functional reusable launch vehicle.

Spaceworks conducted their staging study on certain staging parameters. The study focused on the Mach number leading up to the pull-up maneuver and the velocity at which stage separation takes place. The maximum scramjet Mach number, the Mach number leading up to the pull-up maneuver, and the velocity at which staging occurs were lowered to find the effect on vehicle weight given a fixed payload. The payload weight was provided by Spaceworks for the baseline configuration only (7:4). All calculations for this evaluation maintained the same payload weight provided.

Spaceworks data indicated that lowering the maximum scramjet Mach numbers and the staging velocity lowered the GTOW until a maximum scramjet Mach number of 6 and a staging velocity of 7000 ft/sec was achieved. At a maximum scramjet Mach number of 5 and a staging velocity of 6000 ft/sec, the GTOW increased in weight, but still less than the baseline.

Table 1 is a summary of the findings. The baseline configuration for Quicksat accelerates to Mach 8, at which time, the pull-up maneuver takes place. In all cases studied by Spaceworks, the vehicle uses rocket power assistance to propel the empty weight of the booster, including the upper stage, until the staging velocity (9000 ft/sec).

The optimum maximum scramjet Mach number and staging velocity for this study is the case that has the lightest GTOW as shown in Table 1. Based on the GTOW being 14% lighter than the baseline configuration, as shown in Table 1, the optimum case is when the Mach number is 6 and the staging velocity is 7000 ft/sec. A probable reason for this optimum GTOW is due to the addition of propellant and inert weight. These masses are required by the second stage to provide more velocity to achieve orbit given the fixed payload. This weight gain overtakes the propellant and inert weight saved from having a lower maximum scramjet Mach number and staging velocity by the first stage Quicksat booster.

In conclusion, the data provided by Spaceworks revealed a 14% potential savings in GTOW. These savings were accomplished by lowering the maximum scramjet Mach number and the staging velocity while maintaining payload requirements.

Table 1. Spaceworks Study of Maximum Scramjet Mach Number

| VEHICLE WEIGHT (LBF) | MAXIMUM SCRAMJET MACH NUMBER/ STAGING VELOCITY (FT/SEC) | | | |
|---|--|------------------|-----------------|----------------------|
| | 5 / 6000 | 6 / 7000 | 7 / 8000 | 8 / 9000 BASELINE |
| GTOW (lbf) | 659,131 | 640,323 | 684,308 | 741,670 |
| Difference From Baseline | -82,539 -11% | -101,347 -14% | -57,362 -8% | |
| Stage 1 Dry Weight (lbf) | 142,522 | 142,332 | 154,670 | 167,755 |
| Difference From Baseline (lbf) | -25,203 -15% | -25,423 -15% | -13,085 -8% | |
| 1 st Stage Propellant Weight (lbf) | 373,358 | 377,724 | 434,523 | 484,390 |
| Difference From Baseline (lbf) | -111,032 -23% | -106,666 -22% | -49,867 -10% | |
| 2 nd Stage Total Weight (lbf) | 143,221 | 120,267 | 95,115 | 89,525 |
| Difference From Baseline (lbf) | +53,696 +60% | +30,724 +34% | +5,590 +6% | |
| 2 nd Stage Dry Weight (lbf) | 6,311 | 5,458 | 4,492 | 4,269 |
| Difference From Baseline (lbf) | +2,062 +48% | +1189 +28% | +223 +5% | |
| 2 nd Stage Propellant Weight (lbf) | 123,800 | 101,719 | 77,533 | 72,166 |
| Difference From Baseline (lbf) | +51,634 +72% | +29,553 +41% | +5,367 +7% | |
| Payload Weight (lbf) | 13,090 | 13,090 | 13,090 | 13,090 |

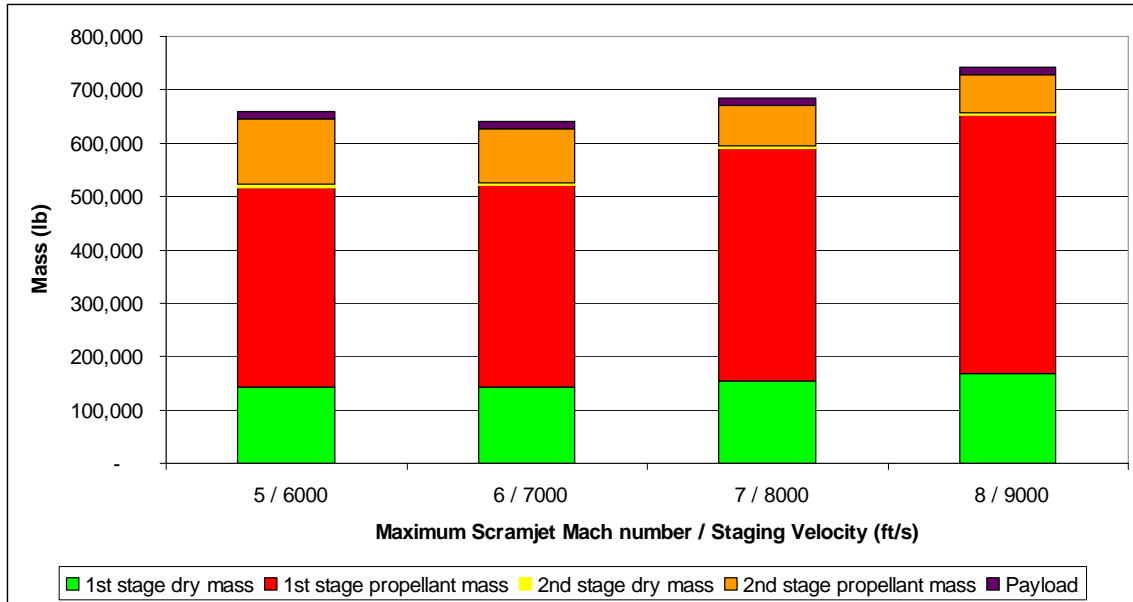


Figure 1. Quicksat weight as a function of maximum scramjet Mach number and staging velocity

III. Methodology

Program to Optimize Simulated Trajectories

Program to Optimize Simulated Trajectories (POST) was developed by NASA as a tool to provide optimal point mass trajectories for various vehicles (9). POST was developed in the 1970s with the purpose of simulating and optimizing trajectories for the Space Shuttle. By 1997, POST was improved by NASA and now offers an enhanced vehicle modeling, trajectory simulation, targeting and optimization capabilities (9:2-1).

For the purposes of this work, POST was used to maximize payload weight by optimizing trajectories while fixing the gross take-off weight (GTOW), inert mass fractions and other parameters for various configurations. One reason for using POST is that it is a well-established program developed and used by NASA. Another reason is that other organizations used POST to optimize trajectories. Finally, due to prior work, variations in staging parameters and their effect on payload can be studied without generating new data files.

Staging is the process by which one set of conditions transitions to another. The transition from turbojet engines to scramjet engines is staging. However, this study focuses on the transition where physical separation takes place. The first upper stage separation from the lower stage is the staging condition being studied. For the rocket-rocket configuration the transition from first stage rocket to second stage rocket is called staging. For the TJ configuration the staging occurs when the configuration transitions from turbojet operation to upper stage rocket operation. For the TBCC configuration

staging occurs when the transition from scramjet first stage to rocket powered second stage takes effect. The transition from turbojet to scramjet is not considered staging due to the lack of physical separation. The transition from second stage rocket booster to final payload insertion is not considered staging due to lack of effect on the payload. Overall, staging is being defined for this study as the physical separation of two bodies.

POST was used in this study as a way to find measurable parameters dealing directly with stage separation. To identify these parameters, three different vehicle configurations were studied. The rocket-rocket (RKT) configuration was selected as a baseline configuration. The RKT configuration represents a potential rocket launch vehicle that could be built today, in order to compare future reusable launch vehicle (RLV) concepts. The turbojet-rocket (TJ) configuration was selected to represent the first generation of air-breathing RLV. The idea behind the TJ configuration is that it does not require scramjet technology in order to be operational. The turbine based combined cycle-rocket (TBCC) configuration was selected as the theoretical scenario. The TBCC uses a combination of scramjet, turbojet and rocket technologies.

Reviewing the input files of these configurations revealed four parameters directly relating to stage separation that affected final payload. The four parameters are coasting time, staging dynamic pressure, staging Mach number and pitch rate. Coasting time is the time delay after the first stage separation, and before the second stage rocket engine firing. Staging dynamic pressure is the dynamic pressure of the vehicle when stage separation occurs. Staging dynamic pressure can be set as a staging condition, as with the TJ and TBCC configurations. The staging dynamic pressure can also be calculated by POST as the dynamic pressure achieved when stage separation occurs. Staging Mach

number is the Mach number, or relative velocity, of the vehicle when stage separation occurs. Staging Mach number can be set as the condition at which staging occurs. The RKT configuration uses staging Mach number as a staging variable, unlike the TJ or TBCC configurations. The staging Mach number can also be calculated by POST as the Mach number achieved when stage separation occurs.

Pitch is a parameter that POST uses in order to control flight trajectory. The use of pitch control requires an estimated pitch rate for various moments throughout the trajectory that was provided in the input file. POST then adjusts those initial estimates for pitch in order to maximize payload.

Input Files

POST requires that input files be created. The input files are the interface between the researcher and the software. The input file is everything the program needs to know in order to perform a successful computational run. The input files for each configuration used for this work originated from the research work of Brock (1).

All input files used in this study begin with establishing constraint variables. Constraint variables are mandatory variables that tell POST how to perform a computational run. The first constraint variable established in each input file used is the input/output unit flag (IOFLAG). It is necessary to ensure all values used are in the same set of units. The units established by Brock, English units, were kept throughout all files to reduce the chance of mixing units. Another constraint variable is the optimization variable (OPT). The OPT constraint variable tells POST what variable(s) to optimize, whether to maximize or minimize the variable(s), and when in the computational run the variable(s) should be optimized.

Parameters are variables (input and output) that do not tell POST how to perform the computational runs. For example, the altitude parameter GDALT is an output parameter noting the altitude of the configuration at a given time. A change in GDALT does not change how POST performs any calculation, but may change the output calculated. Changes in the IOFLAG modify what units POST looks for and how it calculates different values. Constraint variables and parameters differ in how they are used in POST.

Parameters

To effectively compare results from one configuration to another, some parameters were held constant between each vehicle configuration. The first parameter held constant was the launch site at Vandenberg Air Force Base, CA. It was chosen because it allows for polar orbit launches. A polar orbit was preferred because it requires the most Delta V. The relative orbital velocity (25,643 ft/s) and altitude (303,085 ft) describe 50 by 100 mile orbits. For payload sensitivity considerations, the acceleration limit of 3.5 g was established. In order to be consistent, each configuration (RKT, TJ and TBCC) was given the aerodynamic profile of the X-43, Hyper-X. The lift and drag coefficients at varying Mach numbers and angle of attacks for the Hyper-X are presented in Appendix A.

Each configuration required a specific parameter to denote the characteristics of that configuration. As a result, some parameters between the three configurations were different. Those parameters include: inert mass fraction, gross take-off weight (GTOW), first stage engines, staging conditions, baseline staging value, take-off angle, drag

multiplier and the maximum dynamic pressure. Table 2 presents the values of these parameters.

Table 2. Summary of Varied Parameters

| PARAMETERS | RKT | TJ | TBCC |
|---------------------------------|-----------------------------------|------------------------------------|------------------------------------|
| Inert Mass Fraction | 0.1 | 0.35 | 0.30 |
| Initial GTOW | 1,000,000 lbf | 1,000,000 lbf | 800,000 lbf |
| Stage 1 Engine | RD-180 (ISP 370) | AFRL M4.4 TJ | TJ and HRE Scramjet |
| Number of Engines | 2.5 | 12 | 12 TJ and 1 Scramjet |
| Staging Parameter | Mach number | Dynamic pressure | Dynamic pressure |
| Baseline Staging Value | Mach 3.0 | 350 psf | 350 psf |
| Take off Angle | 90 degrees (vertical take-off) | 0 degrees (horizontal take-off) | 0 degrees (horizontal take-off) |
| Drag Multiplier | 0.25 | 0.25 | 1.0 |
| Maximum Dynamic Pressure | 600 psf | 2250 psf | 2250 psf |

A sensitivity study completed by Brock (1) determined that payload for the RKT configuration varied greatly with the first stage inert mass fraction. While an inert mass fraction of 0.17 failed to reach orbit, due to insufficient propellant, an inert mass fraction of 0.1 generated a payload weight of 17,568 lbf (1:38, 54). The first stage inert mass fraction of 0.1 was selected for the RKT configuration based on the nominal range of actual inert mass fractions for various RKT configurations, and the amount of payload generated (1:37-38). Brock concluded that TJ configurations were not sensitive to the

first stage inert mass fraction selected (1). Thus, the first stage inert mass fractions of 0.35 and 0.30 for the TJ and TBCC, respectively, were based on the average value of various air breathing configurations studied by Brock (1:37-39).

The baseline GTOW of all three configurations were previously studied and determined by Brock (1). Brock concluded that most airport runways could support a 1,000,000 pound vehicle. Therefore, the GTOW for each configuration was limited to 1,000,000 pounds. In the case of the TBCC, the weight was reduced to 800,000 pounds to acknowledge the advances in technology, such as lighter materials and more efficient designs.

There are three types of engines being used in this work. Engine data can be incorporated into POST in several different ways. For the rocket engines described below, POST calculates thrust based on a fixed engine thrust and effective exit area. The fuel consumption rate for the RKT, TJ and TBCC engines are calculated by dividing the total thrust by the specific impulse (Isp) of the engines.

Baseline thrust for the turbojet engine is a function of altitude and Mach number as shown in Table 3. The total thrust is generated by multiplying the baseline thrust by the number of engines. The baseline specific impulse for the AFRL turbojet is a function of altitude and Mach number as shown in Table 4. The scramjet engine is incorporated into POST through the use of a thrust coefficient that varies as a function of altitude and Mach number as shown in Table 5. POST calculates total thrust for the scramjet engine by multiplying the thrust coefficient by the dynamic pressure and the exit area.

The first engine is the rocket engine, an RD-180. It is used during the first stage of the RKT configuration, and in the second stage of all three configurations. The RD-

180, currently being used on the Atlas IIAR rockets produced by Lockheed Martin has a specific impulse (Isp) of 337 seconds. An Isp of 370 seconds was used to allow for a 10% increase in future technologies. The thrust provided by each RD-180 is maintained at the current 933,000 lbf thrust (1:42). Advances in future technologies assume a desired thrust is maintained while increasing engine efficiency (Isp). To assure that a 1,000,000 pound GTOW launch vehicle has enough thrust to achieve orbit, the first stage rocket engine is sized to produce over 1.5 million pounds of thrust (1). To generate this thrust, the effective exit area of the engine is increased to about 75 square feet (1). The effective exit area equates to the thrust of two and a half RD-180 engines.

Another engine used in this study is the Mach 4.4 turbojet engine (1:31). This engine's thrust characteristics were provided by the Air Force Research Laboratory (AFRL) as a conceptual turbine accelerator engine (1:42). The Mach 4.4 turbojet engine's thrust characteristics and Isp characteristics are presented in Table 3 and Table 4, respectively.

The Mach 4.4 engine is used by both the TJ and the TBCC configurations in the first stage. The thrust required to overcome the excessive drag generated by the Hyper-X airframe at low Mach numbers was determined to be that of 12 turbojet engines (1:43). The takeoff thrust to weight (T/W) ratio of 0.67 for the 12 turbojet engines was within the range of acceptable of literature reviewed by Brock (1:43).

Table 3. AFRL Mach 4.4 Turbojet Thrust (lbf)

| ALT (FT) | MACH NUMBER | | | | | | | | | | | |
|-------------|-------------|-------|--------|--------|--------|--------|--------|--------|-------|--------|--------|--------|
| | 0 | 0.5 | 0.8 | 1 | 1.5 | 2 | 2.5 | 3 | 3.25 | 3.75 | 4 | 4.4 |
| 0 | 51621 | 54326 | 51785 | 53721 | 74073 | 0 | 0 | 0 | 0 | 0 | 0 | 0 |
| 5,000 | 0 | 47598 | 39940 | 45774 | 65959 | 0 | 0 | 0 | 0 | 0 | 0 | 0 |
| 10,000 | 0 | 0 | 33160 | 38853 | 58108 | 81412 | 127578 | 0 | 0 | 0 | 0 | 0 |
| 20,000 | 0 | 0 | 22508 | 26583 | 42066 | 65315 | 100391 | 146736 | 0 | 0 | 0 | 0 |
| 30,000 | 0 | 0 | 14923 | 17615 | 29340 | 48284 | 71157 | 100641 | 0 | 0 | 0 | 0 |
| 40,000 | 0 | 0 | 9584.4 | 11293 | 19106 | 31506 | 46397 | 65463 | 74388 | 92791 | 103912 | 119178 |
| 42,000 | 0 | 0 | 0 | 10254 | 17324 | 28618 | 42120 | 59417 | 67514 | 84201 | 94279 | 108120 |
| 50,000 | 0 | 0 | 0 | 6966.7 | 11778 | 19448 | 28620 | 40321 | 45834 | 57072 | 63871 | 73190 |
| 60,000 | 0 | 0 | 0 | 4295 | 7270.1 | 11984 | 17650 | 24826 | 28208 | 35084 | 39236 | 44908 |
| 70,000 | 0 | 0 | 0 | 2638.8 | 4479.5 | 7362.4 | 10815 | 15206 | 17256 | 21419 | 23971 | 27422 |
| 72,000 | 0 | 0 | 0 | 2391.9 | 4063.7 | 6669.8 | 9792.5 | 13770 | 15619 | 19403 | 21696 | 24808 |
| 80,000 | 0 | 0 | 0 | 1620.7 | 2748.4 | 4502.2 | 6610.1 | 9293.5 | 10525 | 13053 | 14604 | 16683 |
| 90,000 | 0 | 0 | 0 | 1005 | 1700.8 | 2780.2 | 4071.1 | 5719.5 | 6468 | 8007.4 | 8954.3 | 1234 |
| 100,000 | 0 | 0 | 0 | 627.4 | 1058.2 | 1727.3 | 2526.8 | 3548 | 4003 | 4945.4 | 5535.9 | 6309 |

Table 4. AFRL Mach 4.4 Turbojet Isp (sec)

| ALT (FT) | MACH NUMBER | | | | | | | | | | | |
|-------------|-------------|------|--------|------|--------|--------|------|--------|------|--------|--------|--------|
| | 0 | 0.5 | 0.8 | 1 | 1.5 | 2 | 2.5 | 3 | 3.25 | 3.75 | 4 | 4.4 |
| 0 | 2122 | 1957 | 1765.5 | 1719 | 1605.4 | 0 | 0 | 0 | 0 | 0 | 0 | 0 |
| 5,000 | 0 | 1963 | 1776.4 | 1731 | 1640.8 | 0 | 0 | 0 | 0 | 0 | 0 | 0 |
| 10,000 | 0 | 0 | 1759.1 | 1745 | 1674.3 | 1558.7 | 1563 | 0 | 0 | 0 | 0 | 0 |
| 20,000 | 0 | 0 | 1732.6 | 1731 | 1719.8 | 1671.2 | 1652 | 1605.6 | 0 | 0 | 0 | 0 |
| 30,000 | 0 | 0 | 1717.3 | 1716 | 1765.1 | 1751.7 | 1708 | 1649 | 0 | 0 | 0 | 0 |
| 40,000 | 0 | 0 | 1721.4 | 1718 | 1786.9 | 1780.2 | 1734 | 1676.4 | 1630 | 1534.9 | 1501.1 | 1453 |
| 42,000 | 0 | 0 | 0 | 1717 | 1783.6 | 1779.4 | 1733 | 1675.1 | 1628 | 1533.4 | 1499.4 | 1451.1 |
| 50,000 | 0 | 0 | 0 | 1714 | 1780.9 | 1776.4 | 1729 | 1669.8 | 1623 | 1526.7 | 1492.1 | 1442.8 |
| 60,000 | 0 | 0 | 0 | 1708 | 1777.6 | 1769.5 | 1724 | 1662.6 | 1615 | 1517.6 | 1482.3 | 1431.5 |
| 70,000 | 0 | 0 | 0 | 1702 | 1775 | 1763.2 | 1714 | 1650.8 | 1602 | 1502.7 | 1467.6 | 1415.5 |
| 72,000 | 0 | 0 | 0 | 1701 | 1773.8 | 1760.2 | 1710 | 1647.3 | 1598 | 1498.9 | 1463.7 | 1411 |
| 80,000 | 0 | 0 | 0 | 1694 | 1764.8 | 1747.3 | 1698 | 1633.3 | 1582 | 1481.5 | 1446.8 | 1393.2 |
| 90,000 | 0 | 0 | 0 | 1688 | 1756.2 | 1734.4 | 1681 | 1615.5 | 1563 | 1459.6 | 1424.3 | 1370.6 |
| 100000 | 0 | 0 | 0 | 1681 | 1745.7 | 1720.3 | 1666 | 1598.1 | 1543 | 1437.9 | 1402.5 | 1347 |

The final engine is the scramjet engine. The scramjet technology being suggested for many of the new concepts require high dynamic pressure to initiate and maintain combustion. The X-43 (Hyper-X) developed by NASA was able to ignite and maintain supersonic combustion at 1000 psf (1:1). Scramjet data used in this study, provided by AFRL (1:42), for the Hypersonic Research Engine (HRE) indicate the scramjet can operate down to a dynamic pressure of about 500 psf at a reduced thrust capacity.

The HRE engine was developed by NASA and the USAF in the late 1960s, early 1970s (1:18, 19). Thrust generated by the scramjet engine, for dynamic pressures less than 500 psf, were calculated by POST using the exit area, dynamic pressure and the lowest thrust coefficient provided for a given altitude and Mach number. The exit area and effective number of engines for the scramjet engine were scaled up to 43 times the baseline configuration.

To provide the thrust necessary for acceleration to Mach 8, the exit area is set at 1.5 square feet and the effective number of engines is set to 1.5. Because the data provided by AFRL does not include numbers for the HRE engine below Mach 4, the transition from turbojet mode to scramjet mode was selected as Mach 4. The scramjet operates from Mach 4 to Mach 8. Table 5 indicates that, at a given Mach number, the thrust coefficient increases as dynamic pressure increases.

Thrust, which is a function of the dynamic pressure and thrust coefficient, is greatest at the highest possible dynamic pressure. This engine maintains a constant dynamic pressure of 2250 psf during scramjet combustion to maximize thrust. The Isp values as a function of Mach number and altitude for the scramjet engine are detailed in Table 5.

Table 5. Hypersonic Research Engine-Scramjet Data

| MACH NUMBER | ALTITUDE (FT) | DYNAMIC PRESSURE (PSF) | THRUST COEFFICIENT | ISP (SEC) |
|--------------------|----------------------|-------------------------------|---------------------------|------------------|
| 4 | 56,000 | 2,148 | 0.570 | 1294 |
| | 72,000 | 828 | 0.564 | 1286 |
| | 85,800 | 519 | 0.610 | 1272 |
| 4.5 | 61,500 | 2,141 | 0.693 | 1139 |
| | 76,500 | 1,048 | 0.799 | 1133 |
| | 91,000 | 521 | 0.779 | 1115 |
| 5 | 66,000 | 2,081 | 0.809 | 996 |
| | 80,500 | 1,023 | 1.017 | 981 |
| | 91,500 | 643 | 1.075 | 941 |
| 5.5 | 70,000 | 1,985 | 1.034 | 870 |
| | 84,600 | 981 | 1.099 | 838 |
| | 99,700 | 493 | 1.063 | 813 |
| 6 | 73,500 | 1,865 | 1.022 | 746 |
| | 88,300 | 927 | 1.078 | 723 |
| | 103,500 | 468 | 1.037 | 698 |
| 6.5 | 77,000 | 2,188 | 1.006 | 639 |
| | 92,000 | 1,088 | 1.037 | 615 |
| | 107,000 | 439 | 0.983 | 588 |
| 7 | 80,000 | 2,007 | 0.977 | 538 |
| | 95,050 | 1,003 | 0.955 | 512 |
| | 110,000 | 509 | 0.886 | 479 |
| 7.5 | 83,000 | 1,825 | 0.895 | 438.8 |
| | 98,100 | 916 | 0.848 | 411 |
| | 113,500 | 469 | 0.755 | 369 |
| 8.0 | 85,800 | 2,067 | 0.784 | 342 |
| | 101,000 | 1,043 | 0.705 | 312 |
| | 116,500 | 534 | 0.585 | 261 |
| 8.5 | 88,400 | 1,860 | 0.613 | 245.7 |
| | 104,000 | 939 | 0.553 | 213 |
| | 119,500 | 486 | 0.375 | 153 |

The staging parameter for the RKT configuration was selected as a Mach number. This is result of a traditional direct ascent trajectory that does not rely on dynamic pressure. The baseline value provided by Brock (1) for the RKT configuration is Mach 3. This value was selected based on recommendations provided by AFRL owing to a lack of published data (1:48).

The TJ and TBCC configurations both utilize dynamic pressure when referring to the staging parameter. This is due to the fact that these configurations have to accelerate along high dynamic pressure profiles until the pull-up maneuver occurs. Once this maneuver takes place, the vehicle continues to gain altitude until the dynamic pressure decreased sufficiently for staging to occur. The staging dynamic pressure selected for the baseline TJ and TBCC configuration was based on the upper bound maximum for a staging dynamic pressure range of 200 to 350 psf discovered in a literary sources by Brock (1:47).

The drag coefficient multiplier is a scaling factor of the Hyper-X aerodynamic drag coefficient which is provided in Appendix A. The drag coefficients for the TJ and TBCC configurations were reduced to 25% of the baseline value. The baseline value was reduced because the large drag generated during high dynamic pressure flight prohibited the vehicle from accelerating and gaining altitude (1:40). Lowering the drag coefficient by 75% may not be realistic, and could result in unrealistic design proposals.

The maximum dynamic pressure limits the amount of structural loading and aero-heating incurred during flight. Vehicles with higher inert mass fractions can withstand higher dynamic pressure loading and higher axial acceleration loadings. Typical RKT configurations have a maximum dynamic pressure range of 700 to 2150 psf (1:47). The baseline maximum dynamic pressure for the RKT configuration was selected to be 600 psf. This is because it was “within the range of all the data collected, but was closer to the only source of RLV data” (1:47).

The maximum dynamic pressure for the TJ and TBCC configurations were set to account for the high dynamic pressures desired for the optimal turbojet and scramjet

engines. This means that each configuration either throttled the engine back when the maximum dynamic pressure was attained, as with the RKT configuration, or adjusted pitch to maintain the maximum dynamic pressure for turbojet and scramjet operations.

Pitch Control

The pitch rate is the primary method used by POST for controlling trajectory. When using POST, an initial estimation of pitch rate must be provided in the input file. POST is extremely sensitive to the initial value. If the initial estimation is not close enough to the actual optimized pitch rate, the test may either fail or produce a non-optimized solution, such as overshoot. Small changes in the other variables may influence the validity of the initial pitch rate estimations.

The non-optimized solution could still achieve orbital conditions, but requires more fuel to achieve orbit than in an optimal situation. The most accurate method to determine if the computational run generates an optimal solution is to examine the output file. If the program completed all runs and the data on the optimization parameter is given within specified limits, then the solution is optimal.

Payload

Payload is the weight remaining after the first and second stage propellant and inert weight have either been expelled or separated from the final payload. When GTOW is fixed, the payload becomes the benchmark to compare configurations and staging parameters. The process for determining payload starts with the GTOW.

The vehicle loses propellant based on the thrust generated, divided by the engine I_{sp} , until stage separation occurs. At this point, the vehicle separates weight based on the

inert mass fraction and the propellant consumed during the first stage. Equation (1) is used to calculate inert weight based on an inert mass fraction and propellant consumed.

$$M_i = M_{prop} * (F / (1 - F)) \quad (1)$$

where

M_i = inert weight (lbf)

M_{prop} = propellant weight (lbf)

F = inert mass fraction

After separation and second stage rocket ignition, the vehicle continues to expel weight based on thrust and I_{sp} until final orbital conditions are achieved. The second stage inert weight is calculated based on the inert mass fraction for the second stage and the propellant consumed since first stage separation. Final payload is determined by subtracting the inert weight from the weight of the vehicle when orbital conditions are achieved. If the value remaining is positive then the configuration successfully delivered a payload to orbit.

Accuracy Assessment

The accuracy of POST is based on assessment conducted by Brock (1). The assessment was conducted by using a rocket equation variation Equation (2) to compare against results attained by POST:

$$\Delta V = I_{sp} * g * \ln\left(\frac{W_a}{W_b}\right) - g * (\cos(\theta)) * t_b \quad (2)$$

The modified equations neglect aerodynamic drag and assume constant gravity. The first step in calculating the payload using modified rocket equations was to calculate

the first stage mass using the Equation (3):

$$Wb = \frac{Wo}{\exp\left(\frac{\Delta V + g * [\cos(\theta)] * t}{Isp * g}\right)} \quad (3)$$

The propellant for the first stage was calculated by subtracting the first stage mass from the GTOW. To calculate the inert mass for the first stage use Equation (4):

$$Wi = Wprop * \frac{F}{(1 - F)} \quad (4)$$

The second stage total mass is the end of stage one mass minus the inert mass of stage one. Calculating the weight at orbital insertion is provided in Equation (5):

$$Worb = \frac{Wi2}{\exp\left(\frac{\Delta V + g[\cos(\theta)] * tb}{Isp * g}\right)} \quad (5)$$

The propellant for the second stage is calculated by subtracting the orbital weight from the second stage total weight. The inert mass for the second stage uses the same equation as the first stage. The final payload is the difference between orbital mass and second stage inert mass.

This calculated payload was compared against the data generated by POST in Brock's study. Since the rocket equation used neglected drag, constant gravity, constant flight, and path angle, the values obtained exceed the values calculated by POST.

An assessment of Brock's analysis was within the range of 10%-30% of all tests performed. The data generated by POST was within 10%-30% of the rocket ideals. It can be concluded that POST generates realistic results.

IV. Results and Analysis

Configurations

The rocket-rocket (RKT) configuration was used as the baseline expendable launch vehicle. The flight profile, as shown in Figure 2, of the RKT follows a direct ascent trajectory into orbit. After leaving the launch pad, the vehicle accelerates until the maximum dynamic pressure is reached. The engines are throttled to keep the vehicle from exceeding the maximum dynamic pressure. When the staging Mach number is reached and the first stage inert weight is jettisoned. The vehicle coasts for zero seconds then ignites the second stage rocket engine. The vehicle continues on a direct ascent until orbital velocity and altitude parameters are achieved, the second stage inert weight is jettisoned and the final payload is calculated.

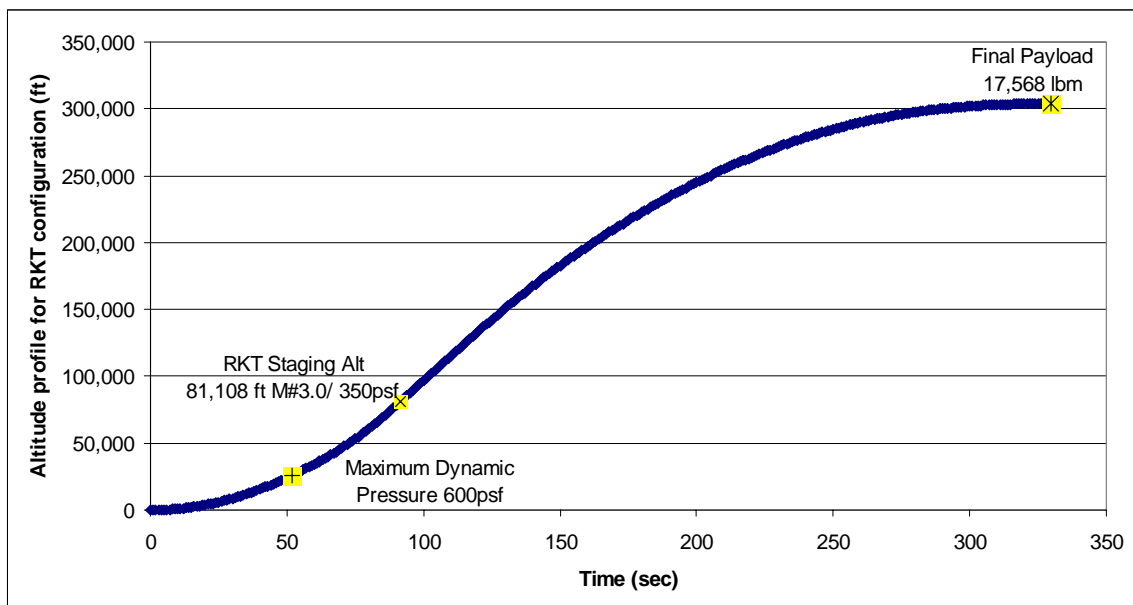


Figure 2. Altitude profile for the RKT configuration as generated by POST

The second configuration is a turbojet-rocket (TJ) configuration. The TJ configuration uses a horizontal take-off horizontal landing (HTHL) a lifting body trajectory as shown in Figure 3. To overcome the excessive drag encountered during low Mach number flight, the TJ configuration used 12 turbojet engines to accelerate along a constant maximum dynamic pressure of 2250 psf up to Mach 4.0 where the pull-up maneuver takes place.

After the pull-up maneuver, the turbojet engines continue to provide thrust while the dynamic pressure drops to staging conditions (baseline 350 psf). However, the thrust provided by the turbojet engines is insufficient to maintain the Mach 4.0 velocity. Therefore, the configuration loses speed while the dynamic pressure decreases.

After staging, the TJ configuration coasts for zero seconds before the RD-180 engine ignites. The second stage then accelerates upward until orbital velocity and altitude are achieved. The second stage inert weight is jettisoned and the final payload weight is calculated.

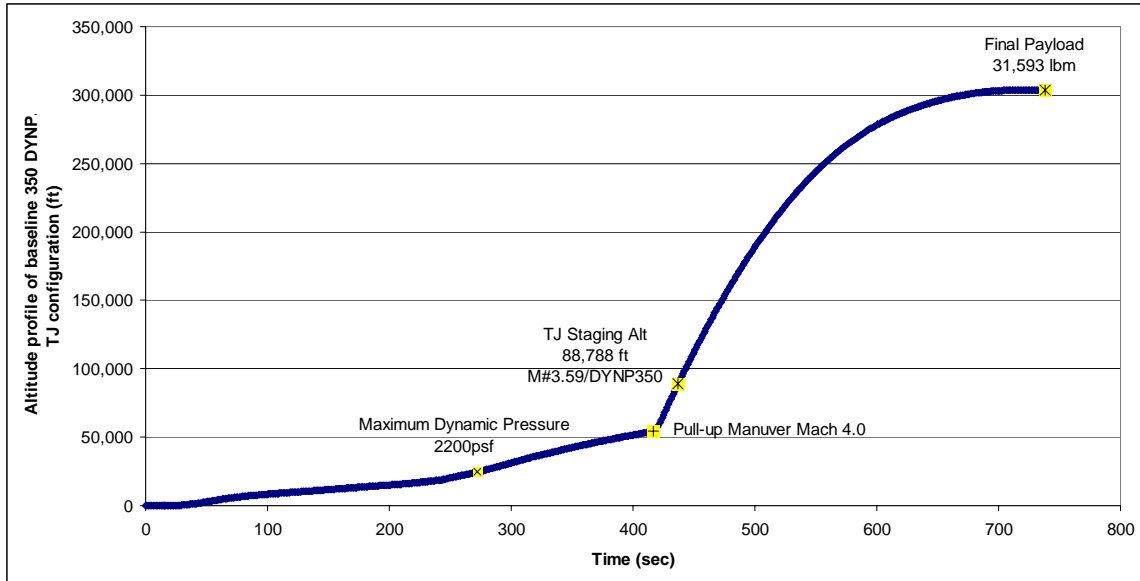


Figure 3. Altitude profile for the TJ configuration as generated by POST

The third configuration studied is the turbine based combined cycle-rocket (TBCC) configuration. Figure 5 details the flight profile of the TBCC configuration. The TBCC used 12 turbojet engines to accelerate the vehicle through the high drag low speed flow to Mach 4. At this point, the TBCC transitions from turbojet engines to the one scaled HRE scramjet engine operation and continues to accelerate the vehicle while maintaining the 2250 psf maximum dynamic pressure until the pull-up Mach number (Mach 8.0) is achieved.

After the pull-up maneuver, the scramjets continue to operate despite the fact that the thrust generated cannot maintain the velocity at Mach 8.0. Prior to the pull-up maneuver, lift is balancing the weight of the vehicle. Figure 4 shows that after the pull-up maneuver the thrust to weight ratio for the vehicle is less than one. The vehicle decelerates until the stage separation occurs and the second stage rocket ignites. This is why the Mach number at staging is always less than the pull-up Mach number.

At the staging dynamic pressure (baseline 350 psf), the scramjet engines are shut down for staging. After staging, the TBCC configuration coasts for zero seconds before the RD-180 engine ignites. The second stage then accelerates upward until orbital velocity and altitude are achieved. The second stage inert weight is jettisoned and the final payload weight is calculated. The transition from turbojet engines to scramjet engines is not being considered due to the lack of physical separation.

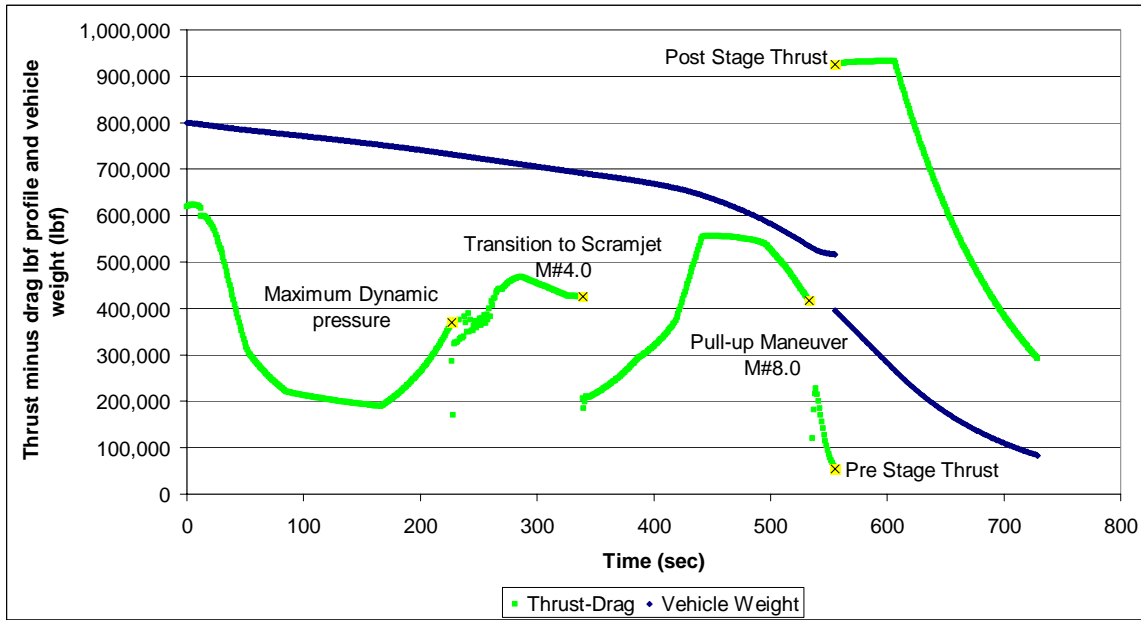


Figure 4. Thrust minus drag vs. weight for baseline TBCC (lbf)

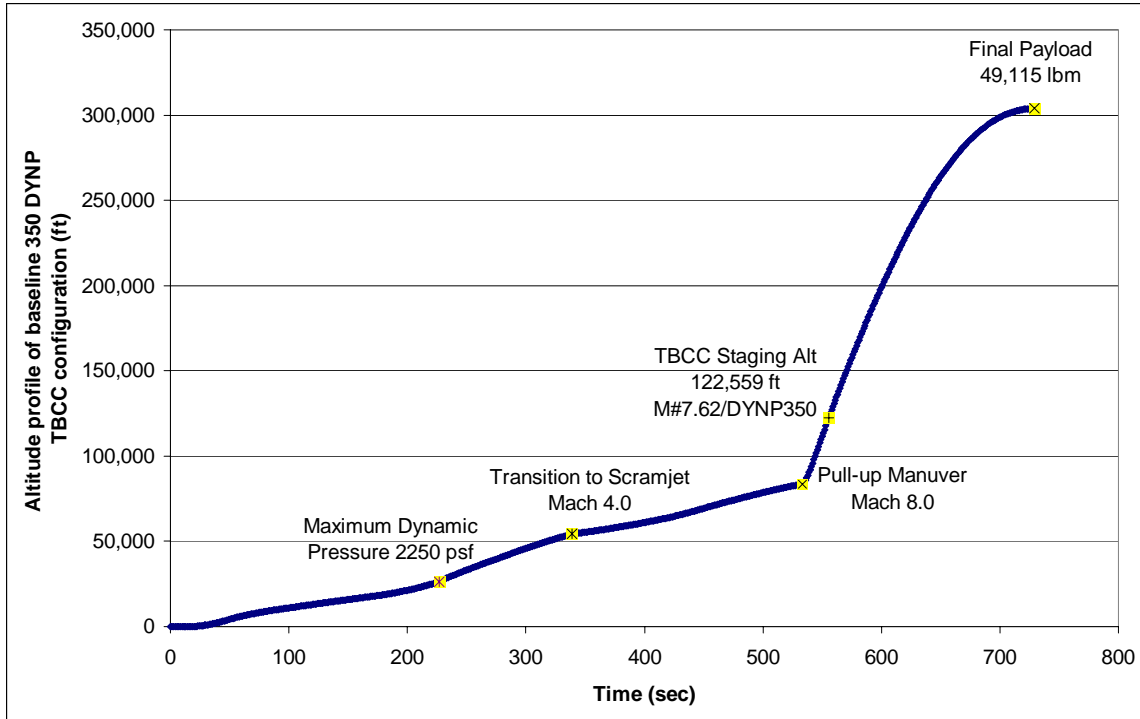


Figure 5. Altitude profile for the TBCC configuration as generated by POST

The differences in each flight profile stem from the way each system reaches orbit. The RKT configuration is a direct ascent (non-lifting trajectory) into space, therefore it reaches orbit the quickest. This does not mean that the RKT is the best configuration, only that it is the quickest to reach orbit. A better indicator as to which configuration is best would be payload weight to orbit and gross take off weight (GTOW). Data from Table 6 suggest that the TBCC is the best configuration due to the high payload weight and low take-off weight.

Table 6. Results of Baseline Configurations

| RESULTS | RKT | TJ | TBCC |
|---------------------------------------|---------------|---------------|-------------|
| Baseline Staging altitude | 81,108 ft | 88,788 ft | 122,559 ft |
| Dynamic pressure | 350 psf | 350 psf | 350 psf |
| Baseline payload weight | 17,553 lbf | 31,594 lbf | 49,115 lbf |
| Stage 1 total weight | 510,527 lbf | 217,039 lbf | 405,133 lbf |
| Stage 1 inert weight | 51,053 lbf | 75,964 lbf | 121,512 lbf |
| Stage 2 total weight | 471,762 lbf | 751,368 lbf | 345,752 lbf |
| Stage 2 inert weight | 47,176 lbf | 75,137 lbf | 34,575 lbf |
| GTOW (fixed provided for ref.) | 1,000,000 lbf | 1,000,000 lbf | 800,000 lbf |

Coasting Time

An often neglected parameter in designing reusable launch vehicles is the coasting time. Coasting time, in this work, is defined as the time it takes from engine shut-off for the first stage to engine ignition of the second stage, during which separation occurs. Except for the US Space Shuttle, all launch systems coast for some length of time while separation takes place.

The study investigates the effect of coasting time during staging on the final payload weight. The idea being that while coasting, the vehicle is losing speed and possibly altitude if the staging is done in horizontal flight and must be made up in terms

of extra fuel burned to reach orbit. The near linear change in payload weight is detailed in Table 7 .

Table 7. Coasting Time Effect on Payload (without fixed altitudes)

| RESULTS | RKT | TJ | TBCC |
|--|------------|-------------|-------------|
| Baseline Staging altitude | 81,108 ft | 88,788 ft | 122,559 ft |
| Coasting 0 seconds payload weight | 17,553 lbf | 31,594 lbf | 49,115 lbf |
| Coasting 1 second payload weight | 17,462 lbf | 31,397 lbf | 49,092 lbf |
| Coasting 2 seconds payload weight | 17,047 lbf | 31,201 lbf | 49,068 lbf |
| Coasting 3 seconds payload weight | 17,333 lbf | 31,003 lbf | 49,044 lbf |
| Coasting 4 seconds payload weight | 17,253 lbf | 30,803 lbf | 49,019 lbf |
| Coasting 5 seconds payload weight | 17,171 lbf | 30,601 lbf | 48,994 lbf |
| Average Penalty Payload weight/second | 73 lbf/sec | 198 lbf/sec | 24 lbf/sec |

It was determined early on that not all configurations reached the same staging parameters when coasting time was added. Table 8 outlines the various parameters and how they changed as coasting time increased.

Table 8. Variation in Staging Conditions as Coasting Time Increased

| RESULTS | RKT | TJ | TBCC |
|------------------------------------|------------|-----------|-------------|
| Baseline altitude | 81,108 ft | 88,788 ft | 122,559 ft |
| relative velocity | 2935 ft/s | 3525 ft/s | 7813 ft/s |
| Coasting 1 second altitude | 81,109 ft | 88,742 ft | 122,546 ft |
| Relative velocity | 2935 ft/s | 3522 ft/s | 7811 ft/s |
| Coasting 2 seconds altitude | 81,109 ft | 88,704 ft | 122,532 ft |
| Relative velocity | 2935 ft/s | 3519 ft/s | 7808 ft/s |
| Coasting 3 seconds altitude | 81,109 ft | 88,665 ft | 122,519 ft |
| Relative velocity | 2935 ft/s | 3516 ft/s | 7806 ft/s |
| Coasting 4 seconds altitude | 81,109 ft | 88,626 ft | 122,506 ft |
| Relative velocity | 2935 ft/s | 3513 ft/s | 7804 ft/s |
| Coasting 5 seconds altitude | 81,109 ft | 88,586 ft | 122,492 ft |
| Relative velocity | 2935 ft/s | 3509 ft/s | 7801 ft/s |

An explanation for this phenomenon is that dynamic pressure is more sensitive to changes in altitude, than Mach number is sensitive to changes in altitude. POST can adjust the pitch so that the vehicle still achieves the same staging dynamic pressures but not achieve the same staging conditions. To rectify this problem, a constraint was added to the TJ and TBCC input files forcing POST to optimize the trajectory to meet not only the staging dynamic pressure requirement but optimize the dynamic pressure at a baseline altitude. Table 9 details the coasting time results while fixing the staging altitudes for each configuration.

Fixing the staging altitude worked very well for the TBCC configuration. Results for the TBCC were linear and consistent. The TJ configuration converged solutions for all runs. When the payload data was calculated, two data results appeared in error.

The payload for the 3 seconds of coasting time and 5 seconds of coasting time for TJ configurations in Table 9, were not consistent with other data. Investigation into the output data indicated that the 3 and 5 seconds of coasting time runs did not meet the orbital requirements as shown in Figure 6. Due to the runs not meeting orbital requirements, the payload data generated was not included in the average payload penalty calculations detailed in Table 9. Pitch control is a potential reason for these runs not meeting orbital conditions. The reason for pitch being the cause of the failed runs is the fact that thrust and velocity were consistent with data from the other runs.

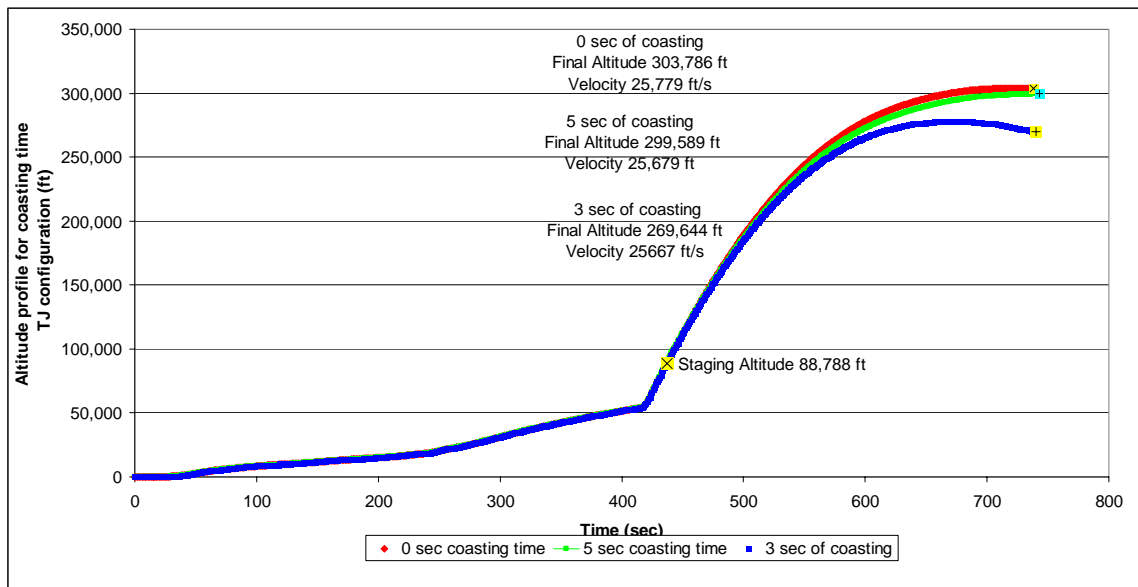


Figure 6. Altitude profile as coasting time increases (TJ configuration)

Table 9. Coasting Time Effects on Payload (with fixed altitudes)

| RESULTS | RKT | TJ | TBCC |
|--|------------|-------------|-------------|
| Baseline Staging altitude | 81,108 ft | 88,788 ft | 122,559 ft |
| Coasting 0 seconds payload weight | 17,553 lbf | 31,585 lbf | 49,115 lbf |
| Coasting 1 second payload weight | 17,462 lbf | 31,415 lbf | 49,111 lbf |
| Coasting 2 seconds payload weight | 17,047 lbf | 31,225 lbf | 49,110 lbf |
| Coasting 3 seconds payload weight | 17,333 lbf | 31,713 lbf | 49,106 lbf |
| Coasting 4 seconds payload weight | 17,253 lbf | 30,852 lbf | 49,101 lbf |
| Coasting 5 seconds payload weight | 17,171 lbf | 28,228 lbf | 49,094 lbf |
| Average Penalty Payload weight/second | 73 lbf/sec | 182 lbf/sec | 4 lbf/sec |

Holding the staging altitude fixed had an effect of reducing the penalty of the coast time during staging. Introducing coasting time had very little effect on the TBCC configuration (less than 5 lbf of propellant weight for every second of coasting time) while the TJ configuration was effected (more than 180 lbf of propellant weight for every second of coasting time) by the addition of coasting time. An explanation of this phenomenon comes from the fact that the TJ configuration spends the most amount of time in the atmosphere after staging.

This is made evident in Figure 7 where even though the TJ configuration stages earlier than the TBCC it reaches orbit at about the same time as the TBCC configuration. Since the weight of the 2nd stage TJ configuration is much heavier than the second stage, the TBCC configuration thrust to weight after staging is much higher for the TJ configuration. The long flight time is due to the lower thrust to weight problems of the TJ configuration. The TBCC configuration has the smallest penalty for coasting time due to the altitude at which staging occurs and the short time it takes to reach orbit after staging.

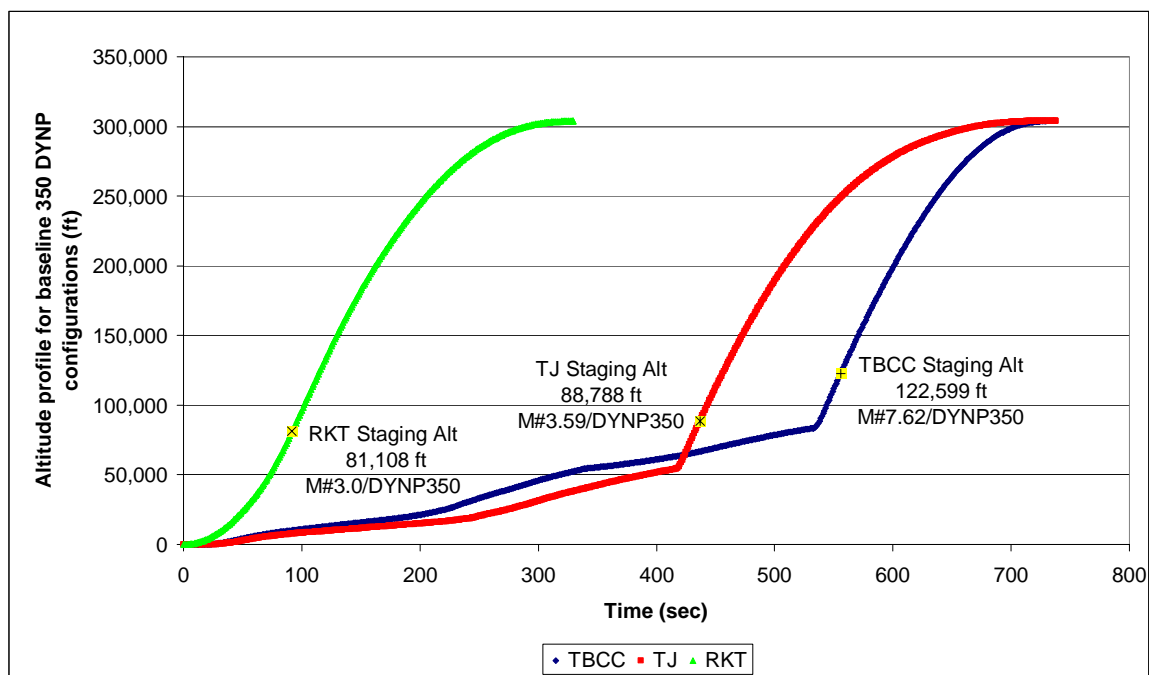


Figure 7. Comparison of altitude profiles for baseline configurations as generated by POST

Overall, the TJ configuration incurred a larger penalty for coasting than the other configurations. At an average of 182 lbf of propellant weight per second of coast time,

the TJ configuration pays over twice the penalty for coasting than a rocket-rocket configuration. This is due to the higher weight at the start of second stage ignition. To overcome the slowing down, the TJ should increase second stage engine thrust. Fixing the staging altitude lowered the penalty on each configuration.

Dynamic Pressure

The purpose of this section is to examine the effect of staging at a high dynamic pressure. The dynamic pressure analysis was conducted solely on the turbine based combine cycle-rocket configuration and the TJ configuration. Recall the RKT configuration used Mach number as a staging condition. Data presented in this section for the RKT configuration were backed out of the staging Mach number analysis and incorporated into this section for completeness.

The study was conducted by modifying input files to stage at various dynamic pressures. The maximum staging dynamic pressure could not exceed the maximum dynamic pressure of 2250 psf. Table 5 indicates that the TBCC can operate at lower dynamic pressures. Figure 4 shows how scramjet engine thrust falls away after pull up stage separation.

The lower limit for the TBCC was established when POST would not converge on a solution with a staging dynamic pressure less than 100 psf. For the TJ configuration, POST would not converge on a solution with a staging dynamic pressure less than 50 psf. The TBCC and TJ configurations are limited in the staging dynamic pressure due to the lack of thrust generated after the configuration performs the pull-up maneuver.

To assure that adjusting the staging dynamic pressure had little impact on actual flight trajectory, the altitude profiles for the TJ and TBCC configurations are shown in

Figure 8 and Figure 9, respectively. Analysis of the charts indicate a trend of increased altitude with lower dynamic pressures and a increase in staging Mach number as stage separation dynamic pressure increases.

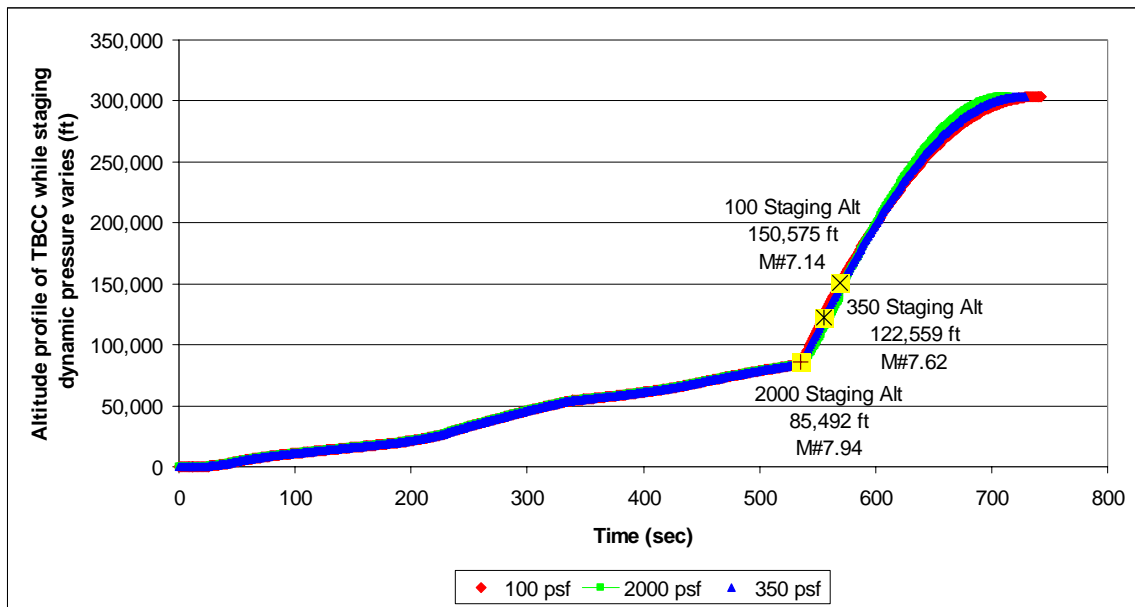


Figure 8. Altitude profile for the TJ configuration as staging dynamic pressure varies

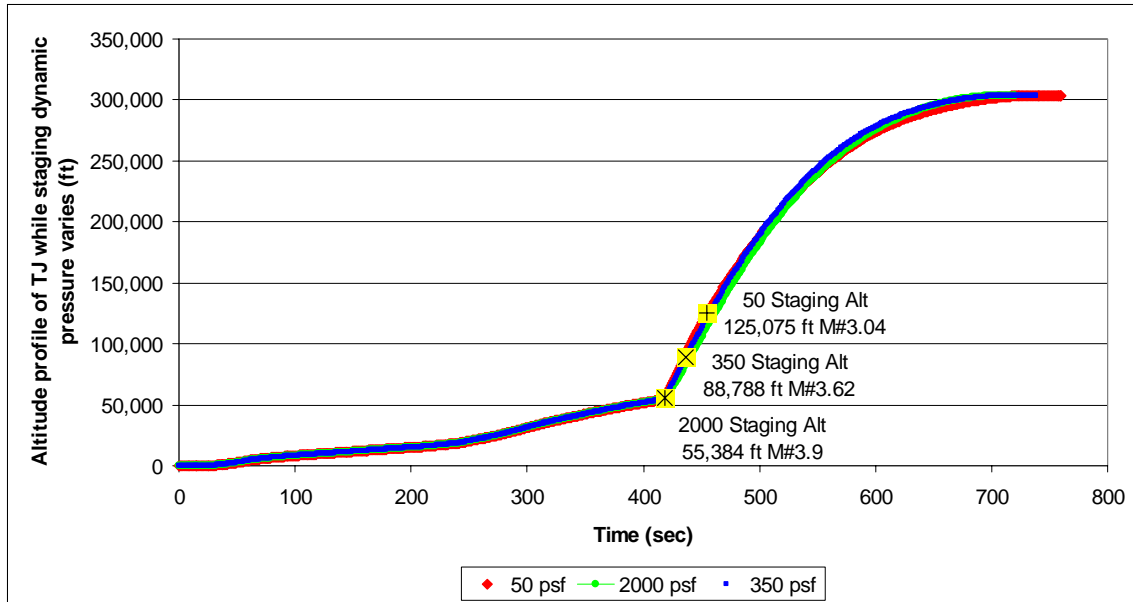


Figure 9. Altitude profile for the TBCC configuration as staging dynamic pressure varies

The payload results of the dynamic pressure runs are summarized in Figure 10. The TBCC configuration produces higher payload than the TJ configuration. A reason for this higher payload capacity by the TBCC configuration lies in the overall efficiency of the design. The increased thrust provided by the scramjet allowed for more payload to be delivered over the TJ and RKT configurations.

This benefit is not affected by the severe loss of negative net thrust to weight ratio after the pull-up maneuver, prior to the stage separation. The TBCC configuration is also less sensitive to staging dynamic pressure than the TJ configuration. The impact of staging dynamic pressure on the final payload is greater for the TJ configuration due to the lower thrust to weight ratio after staging.

In Figure 10 the RKT configuration decreases in payload as staging dynamic pressure increases. This is due to the RKT configuration decreasing in dynamic pressure

as Mach number increases. However, the TJ and TBCC configuration increase in staging dynamic pressure as the staging Mach number increases. Therefore all three configurations increase in payload mass as staging Mach number increases.

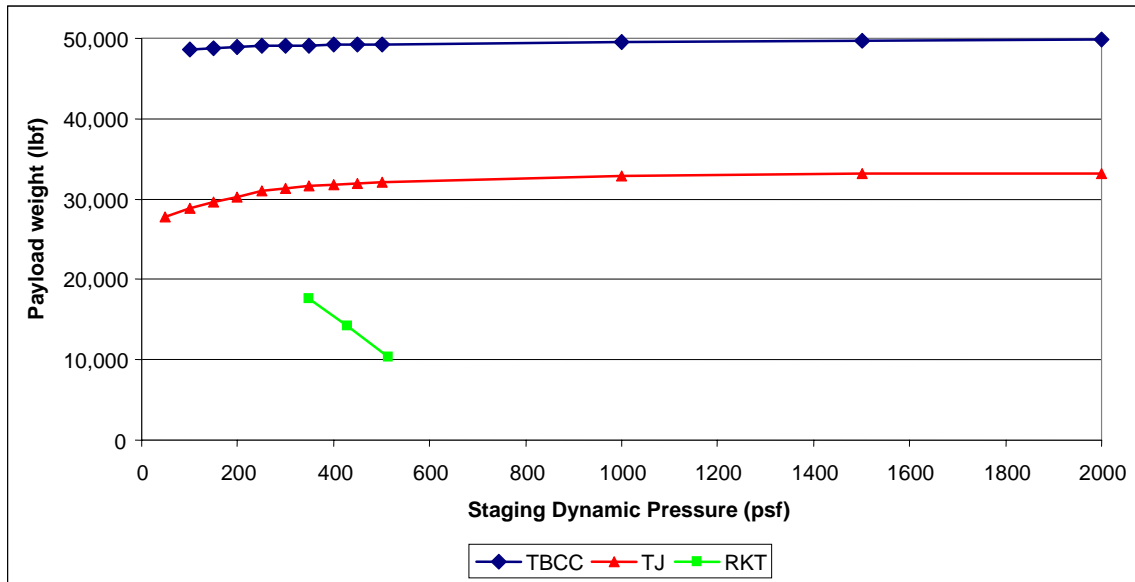


Figure 10. Final payload (stage 3) weight as a function of staging dynamic pressure

The data in Figure 11 indicate a 1.5% increase in payload mass for the TBCC configuration when staging at higher dynamic pressures. Figure 11 shows a trade off in first stage and second stage total mass as staging dynamic pressure increases. The net effect of staging at higher dynamic pressure is an overall increase in payload capacity. The staging dynamic pressure was not tested at the maximum values to account for the time it takes to perform a pull-up maneuver.

Figure 12 illustrates how the TJ configuration gains about 2000 lbf in payload weight when staging dynamic pressure increases. This gain in payload is only 700

pounds for the TBCC configuration. Meaning the TJ configuration benefits the most from increasing staging dynamic pressure.

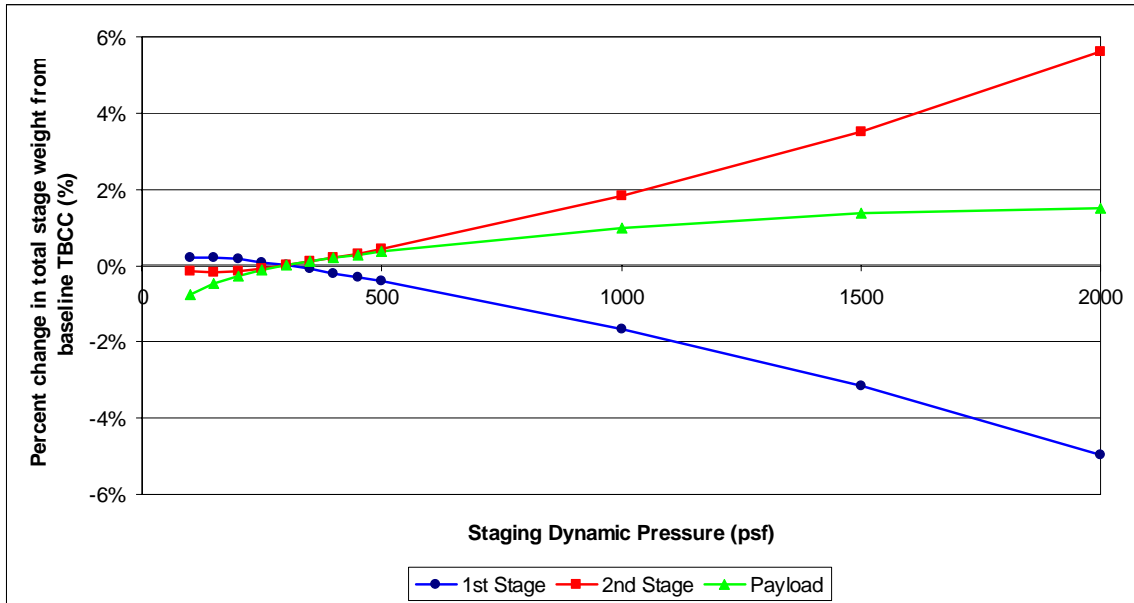


Figure 11. Percent Change in total stage weight from baseline TBCC configuration as staging dynamic pressure varies

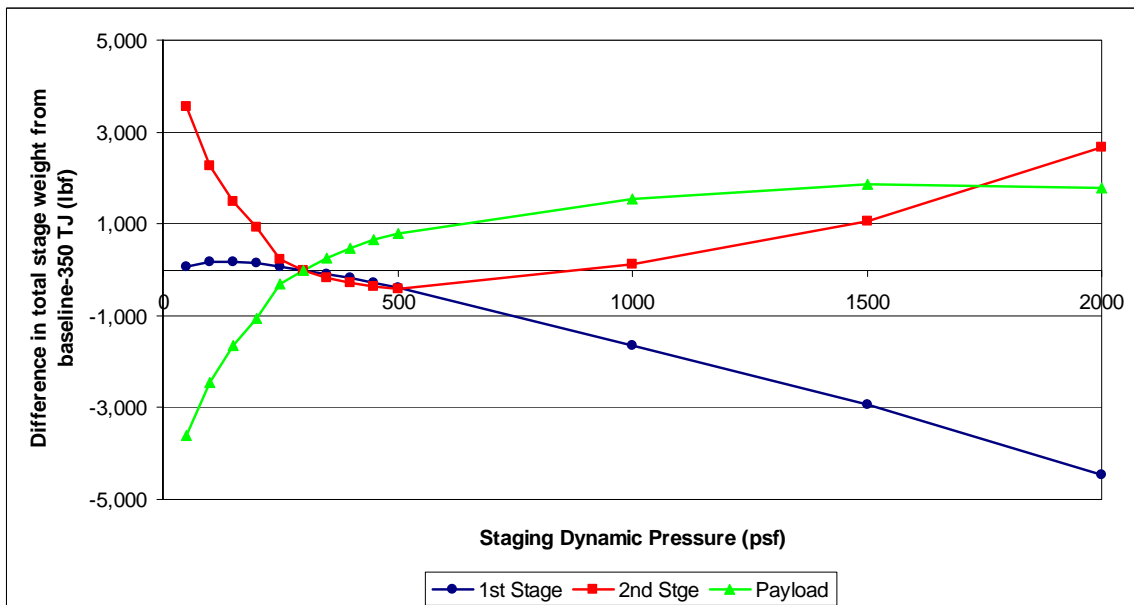


Figure 12. Change in total stage weight from baseline TJ configuration as staging dynamic pressure varies

In conclusion, the data for the TJ and TBCC configurations indicate that staging at higher dynamic pressures, higher Mach number and lower altitudes, generates greater payloads. Staging at a higher dynamic pressure also ensures greater thrust from air breathing engines.

Mach Number

Mach number is used as the staging condition for the Rocket-Rocket (RKT) configuration. The baseline RKT configuration was set for a staging Mach number of 3.0. A staging Mach number range of 2.0 to 4.5 was considered. Runs conducted on the RKT configuration did not converge on a solution for staging Mach numbers above Mach 3.0. It was determined that increasing the GTOW provided the weight for successful computational run convergence. However, this increase in GTOW caused POST to converge on non-optimal (overshoot) trajectory. The data from the overshoot trajectory was used to highlight the sensitivity of POST to the pitch rate. The overshoot trajectory data is represented by the declining rocket-rocket configuration with the GTOW of 1.25 million pounds (RKT 1.25) values within Figure 13.

Data from the staging Mach number sensitivity study conducted by Brock (1:55) was added for comparison. The study used the same fixed parameters and control variables used in this study. The results generated included staging Mach number greater than the baseline staging Mach number of Mach 3. The 0.03% difference in data between the payload calculated in this study, for the Mach 3 case, and the data in Brock's study help validate the data generated in this work.

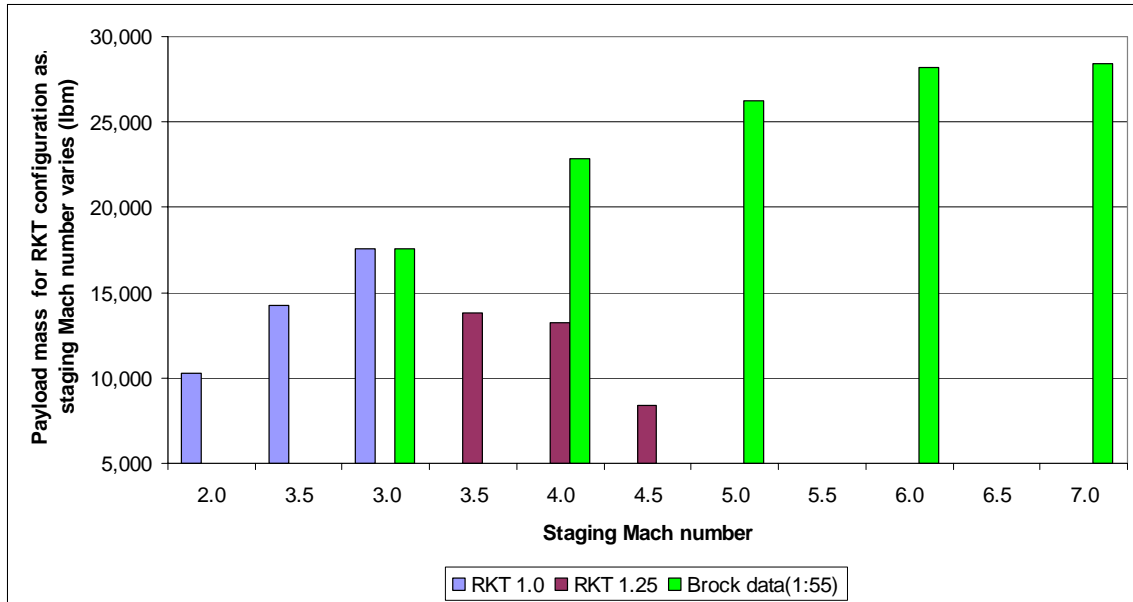


Figure 13. Payload weight for RKT configurations including Brock data (1:55)

The upward trending data in Figure 13 is an indication of payload increase as staging Mach number increases. The trend is not linear. A 7,300 lbf, or 70%, increase in payload weight for increasing the staging Mach number from 2 to 3. An increase of 5,300 lbf, or 30%, in payload weight is attained for staging at Mach 4 versus Mach 3. The trend continues to drop off till the increase is only 240 lbf, or 1%, for going from a staging Mach number of 6 to 7. This implies a maximum improvement in staging Mach number for RKT configurations about Mach 7.

The downward trend of the RKT 1.25 configuration is an indication of the penalty incurred for having an overshoot trajectory. Varying pitch was the method used, in this study, for eliminating overshoot errors on other computational runs. The larger the deviations are from an optimized trajectory, the more fuel is needed to meet orbital requirements. The fuel needed by the overshoot trajectory directly impacts the amount of

payload that would normally be delivered. For example, with a staging Mach number of 4.0, the RKT 1.25 delivered only about a half of the payload of a 20% lighter vehicle using the RKT configuration run by Brock (1:55).

The downward trend in payload weight, as staging Mach number increased, is due to the sensitivity of pitch control to many POST variables. In the RKT configuration pitch control was susceptible to minor changes in GTOW and staging Mach number. Figure 14 shows major deviations from the normal flight profile as a result of changes in GTOW and staging Mach number for the RKT configuration. As staging Mach number increases, the flight profile greatly departs from normal trajectory and performs an overshoot into outer space and recovers to orbital altitude.

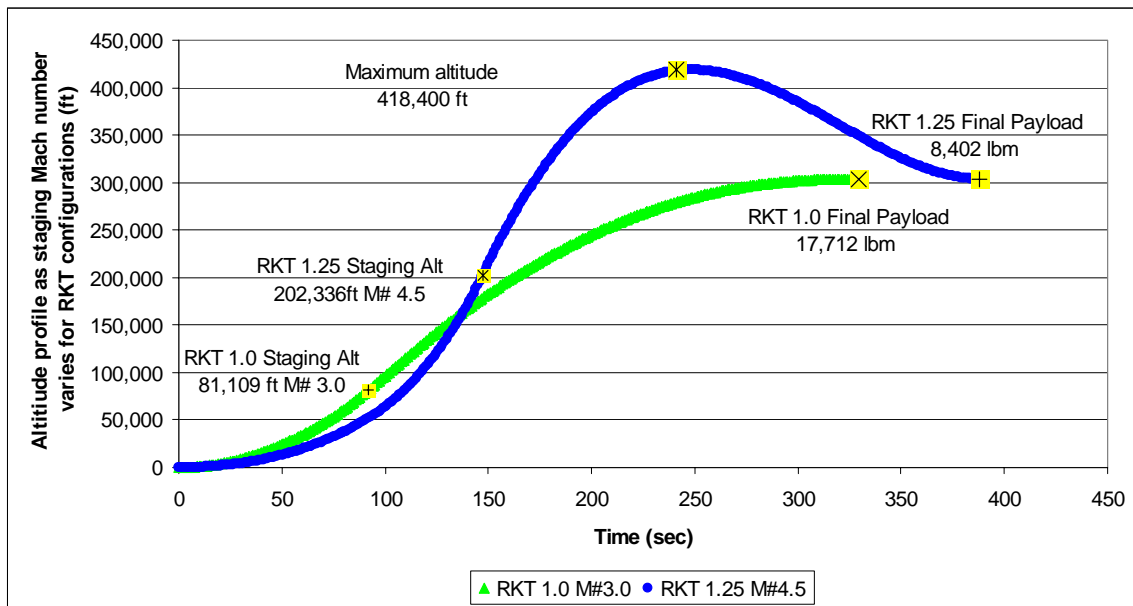


Figure 14. Altitude profile as staging Mach number varies for RKT configurations

The overshoot trajectory impacts the payload for any configuration by necessitating more fuel to propel the vehicle well beyond the desired orbital altitude, before the desired orbital velocity is achieved. Based on the ability to correct the overshoot without having to adjust a fixed parameter, it is recommended to adjust the initial estimation for pitch. This is done by resetting the pitch estimation with the output pitch values calculated by POST and re-running the input file. Having resolved all other issues involving the input file, repeating the computational run with updated pitch values will resolve the overshoot.

Figure 15 is an overview of how staging Mach number affects staging dynamic pressure. In the direct ascent trajectory used by the RKT configuration, Mach number and velocity increase as the RLV leaves the atmosphere. However, as the RKT configuration leaves the atmosphere the dynamic pressure decreases. Figure 13 indicated an increase in payload as staging Mach number increases for the RKT 1.0 configuration. Therefore, the payload increases with a decreasing dynamic pressure. For the TJ and TBCC the increase in staging dynamic pressure as Mach numbers increase is due to the slowing down of the vehicle after the pull-up maneuver.

In conclusion the RKT configuration increases payload as staging Mach number increases. The data in Figure 13 indicated that there is a maximum staging Mach number for RKT configurations around Mach 7.

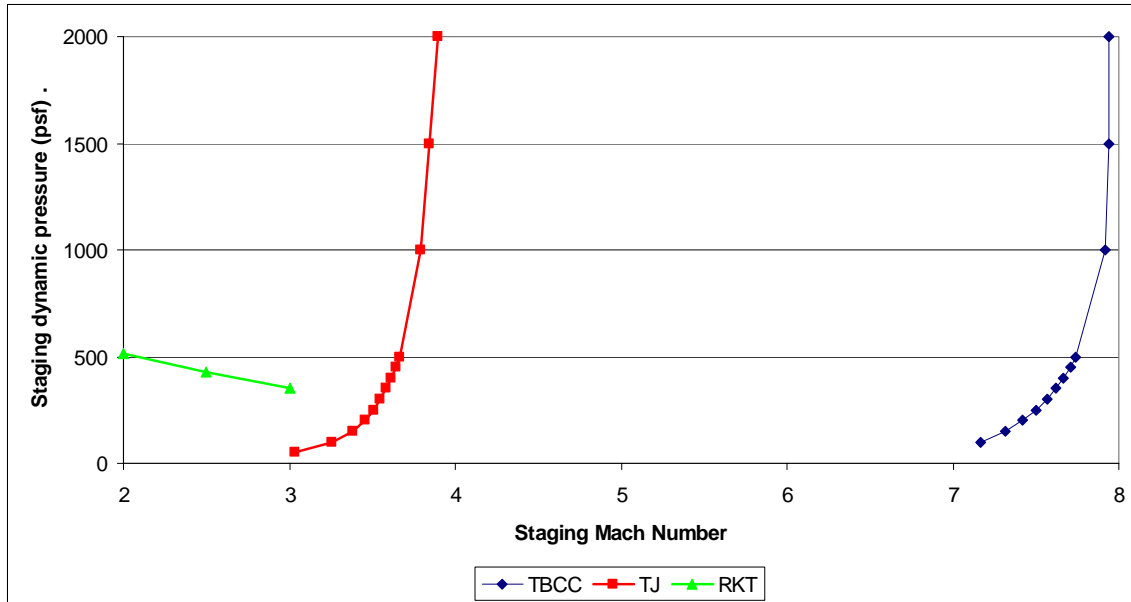


Figure 15. Comparison of staging dynamic pressures vs. staging Mach number

V. Conclusions and Recommendations

Coasting Conclusions

The penalty to payload for coasting time depends on two variables. The first is the altitude at which staging takes place. The second is the thrust to weight ratio for the second stage booster. Increasing thrust reduces the amount of time it takes to get to orbit. Therefore, to minimize coasting penalties, new concepts should stage as high as possible with enough thrust to get the vehicle out of the atmosphere quickly.

Dynamic Pressure Conclusions

Increasing staging dynamic pressure increased the final payload weight as much as 20%, for the TBCC and TJ configuration. Therefore, air breathing TSTO concepts should stage at higher dynamic pressure environments. Increases in staging dynamic pressure decreased the final payload available for the RKT configuration. Due to a maximum difference in payload mass, the TJ configuration had an optimal staging dynamic pressure of 1500 psf. The data in Figure 11 did not show an optimal staging dynamic pressure for the TBCC configuration.

Mach Number Conclusions

All vehicles increased in payload weight as staging Mach number increased. Due to the trending of a maximum Mach number at Mach 7, the optimum staging Mach number for a RKT configuration is Mach 7.

Final Recommendations

As actual field data becomes available for general use, studies focused on advanced RLV concepts need to be updated to assure the assumptions made are accurate and realistic. Work needs to continue in developing accurate scramjet data and tools to predict and control staging of air breathing concepts at high dynamic pressure environments.

Appendix A: X-43 Aerodynamic Properties

| MACH NUMBER | ANGLE OF ATTACK | LIFT COEFFICIENT | DRAG COEFFICIENT |
|--------------------|------------------------|-------------------------|-------------------------|
| 0.3 | -10 | -0.7884 | 0.158016 |
| | -5 | -0.4012 | 0.078816 |
| | 0 | 0.0126 | 0.069 |
| | 5 | 0.4548 | 0.092352 |
| | 10 | 0.7839 | 0.160224 |
| | 15 | 0.9761 | 0.277536 |
| | 20 | 1.0686 | 0.38016 |
| 0.6 | -10 | -0.7884 | 0.158016 |
| | -5 | -0.4012 | 0.078816 |
| | 0 | 0.0126 | 0.069 |
| | 5 | 0.4548 | 0.092352 |
| | 10 | 0.7839 | 0.160224 |
| | 15 | 0.9761 | 0.277536 |
| | 20 | 1.0686 | 0.38016 |
| 0.9 | -10 | -0.7884 | 0.19752 |
| | -5 | -0.4012 | 0.09852 |
| | 0 | 0.0126 | 0.08625 |
| | 5 | 0.4548 | 0.11544 |
| | 10 | 0.7839 | 0.20028 |
| | 15 | 0.9761 | 0.34692 |
| | 20 | 1.0686 | 0.4752 |
| 1.0 | -10 | -0.7884 | 0.2469 |
| | -5 | -0.4012 | 0.12315 |
| | 0 | 0.0126 | 0.08625 |
| | 5 | 0.4548 | 0.1443 |
| | 10 | 0.7839 | 0.25035 |
| | 15 | 0.9761 | 0.43365 |
| | 20 | 1.0686 | 0.594 |
| 1.5 | -10 | -0.7884 | 0.202 |
| | -5 | -0.4012 | 0.1095 |
| | 0 | 0.0126 | 0.0782 |
| | 5 | 0.4548 | 0.1171 |
| | 10 | 0.7839 | 0.2009 |
| | 15 | 0.9761 | 0.3114 |
| | 20 | 1.0686 | 0.4294 |

| MACH NUMBER | ANGLE OF ATTACK | LIFT COEFFICIENT | DRAG COEFFICIENT |
|--------------------|------------------------|-------------------------|-------------------------|
| 2.0 | -10 | -0.5918 | 0.1646 |
| | -5 | -0.2864 | 0.0821 |
| | 0 | 0.0259 | 0.0575 |
| | 5 | 0.3437 | 0.0962 |
| | 10 | 0.6044 | 0.1669 |
| | 15 | 0.8541 | 0.2891 |
| | 20 | 0.9601 | 0.396 |
| 3.0 | -10 | -0.3909 | 0.1123 |
| | -5 | -0.1852 | 0.0549 |
| | 0 | 0.0179 | 0.0389 |
| | 5 | 0.2209 | 0.0632 |
| | 10 | 0.4273 | 0.1293 |
| | 15 | 0.6409 | 0.2421 |
| | 20 | 0.7918 | 0.3544 |
| 4.0 | -10 | -0.3126 | 0.0924 |
| | -5 | -0.1459 | 0.045 |
| | 0 | 0.0156 | 0.0322 |
| | 5 | 0.1769 | 0.0525 |
| | 10 | 0.3438 | 0.1074 |
| | 15 | 0.5193 | 0.2009 |
| | 20 | 0.7054 | 0.3398 |
| 5.0 | -10 | -0.2713 | 0.0817 |
| | -5 | -0.1247 | 0.0394 |
| | 0 | 0.0145 | 0.0282 |
| | 5 | 0.1535 | 0.0465 |
| | 10 | 0.3003 | 0.096 |
| | 15 | 0.459 | 0.1811 |
| | 20 | 0.6297 | 0.3076 |
| 6.0 | -10 | -0.2462 | 0.0755 |
| | -5 | -0.1115 | 0.0361 |
| | 0 | 0.0139 | 0.0259 |
| | 5 | 0.1391 | 0.0431 |
| | 10 | 0.274 | 0.0895 |
| | 15 | 0.4234 | 0.1699 |
| | 20 | 0.587 | 0.2903 |

| MACH NUMBER | ANGLE OF ATTACK | LIFT COEFFICIENT | DRAG COEFFICIENT |
|--------------------|------------------------|-------------------------|-------------------------|
| 8.0 | -10 | -0.2179 | 0.0691 |
| | -5 | -0.0962 | 0.0327 |
| | 0 | 0.0133 | 0.0236 |
| | 5 | 0.1225 | 0.0395 |
| | 10 | 0.2444 | 0.0827 |
| | 15 | 0.3846 | 0.1585 |
| | 20 | 0.542 | 0.2732 |
| 10.0 | -10 | -0.203 | 0.066 |
| | -5 | -0.0879 | 0.0309 |
| | 0 | 0.0131 | 0.0223 |
| | 5 | 0.1136 | 0.0377 |
| | 10 | 0.2288 | 0.0794 |
| | 15 | 0.3649 | 0.1532 |
| | 20 | 0.52 | 0.2656 |
| 12.0 | -10 | -0.1933 | 0.0706 |
| | -5 | -0.0823 | 0.0365 |
| | 0 | 0.0129 | 0.0283 |
| | 5 | 0.1075 | 0.0432 |
| | 10 | 0.2185 | 0.0836 |
| | 15 | 0.3523 | 0.1554 |
| | 20 | 0.5064 | 0.2651 |
| 15.0 | -10 | -0.1848 | 0.0742 |
| | -5 | -0.0774 | 0.0405 |
| | 0 | 0.0127 | 0.0325 |
| | 5 | 0.102 | 0.0473 |
| | 10 | 0.2095 | 0.087 |
| | 15 | 0.3414 | 0.1577 |
| | 20 | 0.4947 | 0.2653 |
| 25.0 | -10 | -0.1753 | 0.0726 |
| | -5 | -0.0714 | 0.0401 |
| | 0 | 0.0128 | 0.0326 |
| | 5 | 0.0954 | 0.0468 |
| | 10 | 0.1997 | 0.0839 |
| | 15 | 0.3304 | 0.1534 |
| | 20 | 0.4828 | 0.2617 |

Bibliography

1. Brock, Mark A. *Performance study of Two-Stage-Two-Orbit Reusable Launch Vehicle Propulsion Alternatives*. MS study AFIT/GSS/ENY/04-M02. School of Engineering and Management, Air Force Institute of Technology (AU), Wright-Patterson AFB OH, March 2004.
2. Murphy, Kelly J. Gary Erickson, and Scott Goodliff. *Experimental Stage Separation Tool Development in NASA Langley's Unitary Plan Wind Tunnel*. AIAA 2004-4727. 22nd Applied Aerodynamics Conference and Exhibit. 16-19 August 2004. Providence, Rhode Island.
3. Reubush, David E. *An Overview of Hyper-X Stage Separation Activities*. JANNAF 35th Combustion/Propulsion Systems Hazards/Airbreathing Propulsion Subcommittees Joint Meeting. 7-11 December 1998. Tucson, Arizona.
4. Buning, Pieter G. Tin-Chee Wong, Arthur D. Dilley and Jenn L. Pao. *Prediction of Hyper-X Stage Separation Aerodynamics Using CFD*. AIAA 2000 4009. 18th Applied Aerodynamics Conference and Exhibit. 14-17 August 2000. Denver, Colorado.
5. Reubush, David E. *Hyper-X Stage Separation Background and Status*. AIAA 99-4818. 9th International Space Planes and Hypersonic Systems and Technologies conference and 3rd Weekly Ionized Gases Workshop. 1-5 November 1999. Norfolk, Virginia.

6. Bradford, J.E. and Eklund, D.R. *Quicksat: A Two-Stage to Orbit Reusable Launch Vehicle Utilizing Air-Breathing Propulsion for Responsive Space Access*. Paper for the American Institute of Aeronautics and Astronautics.
7. Bradfor, J.E D.R *Quicksat TSTO Concept: Baseline Performance Update*. Report for the Air Force Research Lab. February 2004. Wright Patterson Air Force Base, Ohio.
8. Belfior, Michael. "The Five-Billion-Star Hotel," *Popular Science*, March 2005.
9. Powell, R.W. and others. *Program to Optimize Simulated Trajectories (POST)*. NASA Langley Research Center. Hampton, Virginia. 1997.
10. Hill, Philip and Carl Peterson. *Mechanics and Thermodynamics of Propulsion*. Addison-Wesley Publishing Company. Reading, Massachusetts. 1992.

Vita

Lieutenant James K. Nilsen graduated from Steilacoom High School in Steilacoom, Washington. He entered undergraduate studies at the University of Arizona in Tucson, Arizona where he graduated with a Bachelor of Science Degree in Aerospace Engineering in May 1996. He was commissioned through Officer Training School at Maxwell Air Force Base in Montgomery, Alabama in June 2001.

His first assignment was with the 4th Space Operations Squadron, Schriever AFB, Colorado where he served as an Electrical Power Distribution System and Thermal Protection System Engineer for the Milstar satellite constellation. In August 2003, he entered the Graduate School of Engineering and Management, Air Force Institute of Technology. Upon graduation, he will be assigned to the National Air and Space Intelligence Center.

| REPORT DOCUMENTATION PAGE | | | <i>Form Approved OMB No. 074-0188</i> | | |
|---|---------------|---|---|--|--|
| <p>The public reporting burden for this collection of information is estimated to average 1 hour per response, including the time for reviewing instructions, searching existing data sources, gathering and maintaining the data needed, and completing and reviewing the collection of information. Send comments regarding this burden estimate or any other aspect of the collection of information, including suggestions for reducing this burden to Department of Defense, Washington Headquarters Services, Directorate for Information Operations and Reports (0704-0188), 1215 Jefferson Davis Highway, Suite 1204, Arlington, VA 22202-4302. Respondents should be aware that notwithstanding any other provision of law, no person shall be subject to a penalty for failing to comply with a collection of information if it does not display a currently valid OMB control number.</p> <p>PLEASE DO NOT RETURN YOUR FORM TO THE ABOVE ADDRESS.</p> | | | | | |
| 1. REPORT DATE (DD-MM-YYYY) Grad date 21-03-2005 | | 2. REPORT TYPE Master's Thesis | | 3. DATES COVERED (From - To) 27 Aug 2004 - 21 Mar 2005 | |
| 4. TITLE AND SUBTITLE Performance Study of Staging Variables on Two-Stage-To-Orbit Reusable Launch Vehicles | | | 5a. CONTRACT NUMBER | | |
| | | | 5b. GRANT NUMBER | | |
| | | | 5c. PROGRAM ELEMENT NUMBER | | |
| 6. AUTHOR(S) Nilsen, James, K., First Lieutenant, USAF | | | 5d. PROJECT NUMBER If funded, enter ENR # | | |
| | | | 5e. TASK NUMBER | | |
| | | | 5f. WORK UNIT NUMBER | | |
| 7. PERFORMING ORGANIZATION NAMES(S) AND ADDRESS(S) Air Force Institute of Technology Graduate School of Engineering and Management (AFIT/EN) 2950 Hobson Way WPAFB OH 45433-7765 | | | 8. PERFORMING ORGANIZATION REPORT NUMBER AFIT/GA/ENY/05-M08 | | |
| 9. SPONSORING/MONITORING AGENCY NAME(S) AND ADDRESS(ES) AFRL/PRAS 1950 Fifth St. WPAFB OH 45433-7125 DSN: 785-0303 | | | 10. SPONSOR/MONITOR'S ACRONYM(S) | | |
| | | | 11. SPONSOR/MONITOR'S REPORT NUMBER(S) | | |
| 12. DISTRIBUTION/AVAILABILITY STATEMENT APPROVED FOR PUBLIC RELEASE; DISTRIBUTION UNLIMITED. | | | | | |
| 13. SUPPLEMENTARY NOTES | | | | | |
| 14. ABSTRACT The purpose of this research is to investigate the effects of staging variables on Two-Stage-To-Orbit reusable launch vehicles, specifically, the question of what measurable factors play important roles in staging performance. Three different configurations (Rocket-Rocket, Turbojet-Rocket and Turbine Based Combined Cycle-Rocket) were considered. The software, Program to Optimize Simulated Trajectories (POST), was used to analyze these configurations. Vehicle coasting time, staging dynamic pressure and staging Mach number were all varied to determine their influence on the final payload. | | | | | |
| 15. SUBJECT TERMS Staging, Dynamic Pressure, Mach number, Two-Stage-To-Orbit, Reusable Launch Vehicle, Scramjet, Turbojet, Rocket, Coasting time, Pitch Control | | | | | |
| 16. SECURITY CLASSIFICATION OF: | | 17. LIMITATION OF ABSTRACT UU | 18. NUMBER OF PAGES 65 | 19a. NAME OF RESPONSIBLE PERSON Dr. Milton E. Franke | |
| REPOR T U | ABSTRACT U | | | c. THIS PAGE U | 19b. TELEPHONE NUMBER (Include area code) (937) 255-6565; e-mail: Milton.Franke@afit.edu |

Standard Form 298 (Rev: 8-98)

Prescribed by ANSI Std. Z39-18